Potent, Selective, and Orally Efficacious Antagonists of Melanin-Concentrating Hormone Receptor 1

Francis X. Tavares,*[,†] Kamal A. Al-Barazanji,[‡] Eric C. Bigham,[§] Michael J. Bishop,[†] Christy S. Britt,[‡] David L. Carlton,[||] Paul L. Feldman,[†] Aaron S. Goetz,[⊥] Mary K. Grizzle,[‡] Yu C. Guo,[†] Anthony L. Handlon,[†] Donald L. Hertzog,[†] Diane M. Ignar,[‡] Daniel G. Lang,[#] Ronda J. Ott,[⊗] Andrew J. Peat,[†] and Hui-Qiang Zhou[†]

Department of Medicinal Chemistry, Department of Metabolic Diseases, Pharmaceutical Development, Department of Research Bioanalysis and Drug Metabolism, Discovery Research CASS, Department of Biochemical and Analytical Pharmacology, and Screening and Compound Profiling, GlaxoSmithKline, Research Triangle Park, North Carolina 27709

Received May 13, 2006

The high expression of MCH in the hypothalamus with the lean hypophagic phenotype coupled with increased resting metabolic rate and resistance to high fat diet-induced obesity of MCH KO mice has spurred considerable efforts to develop small molecule MCHR1 antagonists. Starting from a lead thienopyrimidinone series, structure−activity studies at the 3- and 6-positions of the thienopyrimidinone core afforded potent and selective MCHR1 antagonists with representative examples having suitable pharmacokinetic properties. Based on structure−activity relationships, a structural model for MCHR1 was constructed to explain the binding mode of these antagonists. In general, a good correlation was observed between pK_as and activity in the right-hand side of the template, with Asp123 playing an important role in the enhancement of binding affinity. A representative example when evaluated chronically in diet-induced obese mice resulted in good weight loss effects. These antagonists provide a viable lead series in the discovery of new therapies for the treatment of obesity.

Introduction

Melanin-concentrating hormone (MCH[a]) is a cyclic nonadecapeptide displaying high sequence conservation in the ring structure with the salmon counterpart from which it was originally isolated.[1a,b] In mammals, MCH is generated via post-translational cleavage of Arg145−Arg146 site by proconvertases in the hypothalamic neurons. Isolation of MCH spurred efforts resulting in identification of its receptor MCHR1 (SLC-1/GPR24) using reverse pharmacology techniques. Recently, a second receptor, MCHR2, with a 38% overall homology and 44% amino acid identity, was identified to MCHR1.[1e] Like MCHR1, MCHR2 also belongs to the rhodopsin family of G-protein-coupled receptors. Key elements of both receptors include a 7-transmembrane (7TM) motif, N-linked glycosylation sites in the N-terminal region that are important for full activity, an aspartic acid−arginine−tyrosine motif located in the cytosolic region of helix 3 (TM3) region and Asp123 and Asp113 in the TM3 regions of MCHR1 and MCHR2, respectively, that may be involved in ligand binding. MCHR1 is expressed in all mammals in contrast to MCHR2, which is present in dogs, ferrets, primates, and humans but absent in rodents.[1e] MCHR1 has been found to couple to Gαi, Go, and Gαq proteins, activating diverse signaling pathways, whereas MCHR2 is exclusively coupled to Gαq proteins.[1f−i] Both receptors have a similar distribution in the CNS.

The high expression of MCHR1 in hypothalamic ventromedial and dorsomedial regions was of particular interest as these regions regulate feeding behavior and energy expenditure.[1c,d] Several reports suggest that MCH plays an important role in energy homeostasis. Genetic manipulations have shed light on the role of MCH in energy homeostasis. MCH-deficient mice have reduced body weight and leanness due to hypophagia and increased metabolic rate when compared to their wild-type littermates.[2a] MCHR1(−/−) mice are resistant to high-fat, diet-induced obesity. These mice are hyperphagic and hypermetabolic with lower levels of insulin and leptin.[2b,c] The differences in feeding behavior between MCH-deficient and receptor knockout mice probably results from deletion of peptides that are generated from preprohormone MCH processing by proconvertases.[2d,e] Transgenic overexpression of MCH in the lateral hypothalamus results in mice being obese, hyperlepitimic, and hyperinsulinemic with islet hyperplasia.[2f] MCH deficiency in ob/ob mice results in dramatic reduction in body fat. These mice show increased basal metabolic temperature, lower plasma glucocorticoid levels, improved glucose tolerance, and reduced expression of stearoyl-CoA desaturase.[2g]

Apart from genetic modifications to the receptor or the MCH gene itself, obese phenotypic models such as obese Zucker rats and ob/ob mice exhibit high hypothalamic levels of MCH.[3a−c] There are several reports studying the effects of intracerebroventricular (ICV) injection of MCH.[3d−g] ICV infusion of MCH in mice on a moderately high fat diet results in increased body weight accompanied by hyperphagia and significant increases in fat and liver weights. Expression levels of key modulators of energy expenditure in brown adipose tissue such as acyl-CoA oxidase, carnitine palmitoyltransferase, and uncoupling protein-1 were also down regulated. In addition, plasma glucose, insulin and leptin levels were increased.[3d,e] Decreased energy expenditure has also been explained by the reduction of plasma thyroid stimulating hormone (TSH) after ICV administration of MCH in rats.[3f] Exogenous administration of MCH to

* To whom correspondence should be addressed. Phone: (919) 483-7456. Fax: (919)-483-6053. E-mail: fxt66911@gsk.com.
[†] Department of Medicinal Chemistry.
[‡] Department of Metabolic Diseases.
[§] Discovery Research CASS.
[||] Pharmaceutical Development.
[⊥] Screening and Compound Profiling.
[#] Department of Biochemical and Analytical Pharmacology.
[⊗] Department of Research Bioanalysis and Drug Metabolism.
[a] Abbreviations: TSH, thyroid stimulating hormone; NPY, neuropeptide Y; α-MSH, α-melanocyte stimulating hormone; DIO, diet-induced obese; hERG, human ether-a-go-go-related gene.

10.1021/jm060572f CCC: $33.50
Published on Web 11/04/2006

hypothalamic explants has been shown to increase the release of orexigenic neurotransmitters such as NPY and Agouti-related protein and decrease the release of anorectic neurotransmitters, α-melanocyte stimulating hormone (α-MSH) and cocaine- and amphetamine-regulated transcript.[3h] The orexigenic action of MCH has been suggested to be mediated via the NPY Y(1) receptor and be independent of galanin and melanocortin receptors.[3i,j] Interactions of MCH containing neurons with other neurons containing orexin may influence food intake through synapse with each other.[3k] Besides insulin secreting cells,[3l] functional MCHR1 receptors are also present in adiposites, because rat adiposites treated with MCH result in the upregulation of leptin, a key cytokine involved in energy homeostasis.[3m]

Although MCHR1(−/−) mice have desirable body weight loss, adverse physiological changes that may limit the use of an MCH antagonist as an antiobesity drug need to be addressed. For example, the knockout mice seem to have increased sympathetic tone resulting in an increased heart rate.[4a] In addition, the MCH knockout mice also show an osteoporotic phenotype due to a high bone turnover.[4b] Although extensive work in rodents has implicated this gene in obesity, to date, linkage of genetic defects causing severe human obesity needs to be established.[4c,d]

Several reports involving the genetic modifications or endogenous administration of MCH have validated MCHR1 to be an important player in energy homeostasis. The orexigenic actions of MCH have been known to be antagonized by endogenous α-MSH.[5a] Early reports regarding the development of MCHR1 antagonists described peptidic compounds that attenuated orexigenic effects of the agonist.[5b−d] Recent reports regarding the use of selective small molecule antagonists have been disclosed. The use of (−)-*N*-[6-(dimethylamino)methyl]-5,6,7,8-tetrahydro-2-naphthalenyl-4′-fluoro[1,1′-biphenyl]-4-carboxamide **55** (T-226296), an orally bioavailable small molecule antagonist of MCHR1, has been shown to suppress MCH stimulated food intake over 90% versus control rats.[5e] Further evaluation of **55** in diet-induced obese (DIO) mice has shown significant weight loss of about 15% at 30 mg/kg in mice on a high fat diet, and these mice were hypophagic.[5f] (+)-Methyl (4*S*)-3-([(3-[4-(3-[acetylamino]phenyl)-1-piperidinyl]propyl)amino]carbonyl)-4-(3,4-difluorophenyl)-6-(methoxymethyl)-2-oxo-1,2,3,4-tetra-hydro-5-pyrimidinecarboxylate hydrochloride (SNAP-7941), another small molecule antagonist, was also shown to decrease food intake, decrease body weight, and block the onset of diet-induced obesity in mice on a high fat diet.[5g] Efforts from other laboratories have also identified 2-amino quinoline analogues as MCHR1 antagonists.[5h−m] In addition, several recent reports on the effects of small molecule MCHR1 antagonists in DIO mice have been described.[6] Recent studies evaluating the role of MCHR1 in the presence of MCHR2 in rhesus monkeys indicate that there was no compensation by MCHR2 on antagonism of MCHR1.[8] In this study, weight loss was observed in the range of 12−16.7% on administration of the MCHR1 antagonist via oral gavage at 7.5 and 15 mg/kg with reduction in food intake. Furthermore, as MCH decreases TSH levels, T4 levels measured in the study were higher than control animals.[8]

Synthetic efforts from these laboratories started from a thienopyrimidinone lead. The aim was to optimize substituents at the 3- and 6-position of the thienopyrimidinone ring system to afford compounds that might be suitable for evaluation in a diet induced obese model. Compounds exhibited potency at the human MCHR1 in CHO Gal4/Elk1-Luc$^+$ reporter assay with no quantifiable activity observed at the untransfected host cell line after stimulation with thrombin, indicating their specificity for MCHR1. In addition, compounds did not have quantifiable activity at the MCHR2 indicating their selectivity for MCHR1. Representative compounds that exhibited functional antagonism at the MCHR1 receptor were progressed into a suitable pharmacokinetic model. Because human ether-a-go-go-related gene (hERG) channel inhibition at times can be a major issue for compounds that interact with 7TM receptors, compounds that were being evaluated for in vivo efficacy were also tested against the hERG channels. Studies regarding evaluation of a representative example in a DIO model will also be described.

Scheme 1. Synthetic Route to Targets **3a**−**3k**[a]

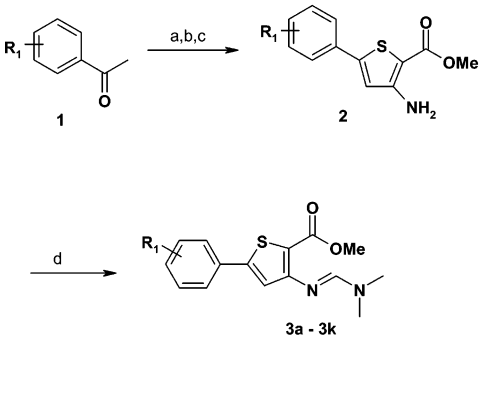

Cmpd	R_1
3a	H
3b	4-Cl
3c	3-Cl
3d	2-Cl
3e	4-Br
3f	4-F
3g	4-CN
3h	4-CF_3
3i	4-OMe
3j	4-^{i}Bu
3k	4-^{t}Bu

[a] Reagents and conditions: (a) DMF/$POCl_3$, rt; (b) NH_2OH·HCl, 0−100 °C; (c) methyl mercaptoacetate, NaOMe, DMF, O °C; (d) $(CH_3O)_2CHNMe_2$, 90 °C, 2 h.

Scheme 2. Synthetic Route to Targets **14**−**39**[a]

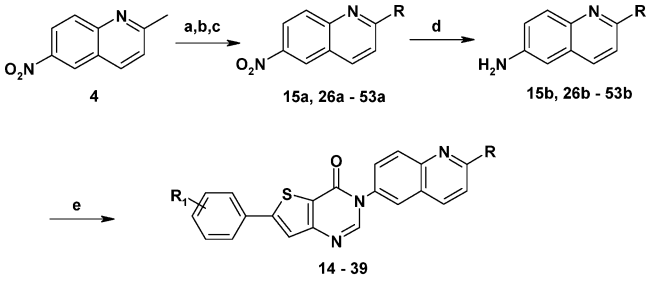

[a] Reagents and conditions: (a) NBS, CH_3CN, 70 °C, 16 h; (b) $(EtO)_2PH$, Et_3N; (c) CH_2Cl_2, amine, Hunig's base; (d) 10% Pd/C, H_2, 40 psi, 6 h; (e) **3a**−**k** (**14**−**24**); **3b** (**25**−**40**), PhOH, 100−135 °C.

Chemistry

The access to the thienopyrimidinone core involved the synthesis of methyl 5-aryl-3-{[(1*E*)-(dimethylamino)methylidene]amino}-2-thiophenecarboxylates **3a**−**k** from commercially available aryl ketones **1**. As shown in Scheme 1, aryl ketones **1** were sequentially treated with DMF/$POCl_3$ and hydroxylamine, followed by the addition of methyl mercaptoacetate, to afford the substituted thiophene esters **2**. The thiophene esters **2**, on treatment with *N*,*N*-dimethyl-1,1-bis(methyloxy)methanamine, afforded the key intermediates, methyl 5-aryl-3-{[(1*E*)-(dimethylamino)methylidene]amino}-2-thiophenecarboxylates **3a**−**k**. The general synthesis of substituted thienopyrimidinones containing a quinoline group is shown in Scheme 2. Bromination of 2-methyl-6-nitro quinoline **4** with NBS afforded a mixture of mono and dibromo compounds, which on treatment with diethyl phosphite[7] in the presence of a base afforded 2-(bromomethyl)-6-nitroquinoline, and subsequent displacement of the bromide with amines afforded the nitro amines **15a** and **26a**−

Table 1. Inhibitory Potencies (IC_{50}) vs hMCHR1[a]

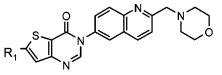

Cmpd	Structure (R_1)	IC_{50} (nM)
14		794
15		4.9
16		3980
17		1258
18		40
19		501
20		478
21		36
22		31
23		200
24		501

[a] Antagonism of human MCHR1 in CHO Gal4/Elk1-Luc$^+$ reporter assay. IC_{50} values represent averages of 2−3 experiments, with a standard deviation of 3-fold.

53a. Reduction of the nitro group with Pd/C under hydrogen afforded the amines **15b** and **26b**−**53b**. Subsequent treatment with methyl 5-aryl-3-{[(1*E*)-(dimethylamino)methylidene]amino}-2-thiophenecarboxylates **3a**−**k** afforded analogues **14**−**24**. Compounds in Table 2 were synthesized by the treatment of **3b** with the respective amino compounds **27b**−**40b** to afford analogues **25**−**40**. The synthesis of analogue **41** is shown as in Scheme 3. Oxidation of the methyl group in 2-methyl-6-nitroquinoline with selenium dioxide afforded the intermediate 6-nitroquinoline-2-carbaldehyde **5**. Reduction of the aldehyde group in **5** with sodium borohydride afforded the alcohol **6**. Protection of the alcohol **6** using *tert*-butyldimethylsilyl chloride, followed by sequential reduction, cyclization, and deprotection gave analogue **41**.

Analogues **42**−**49** containing the dihydobenzoxazine moiety involved synthetic manipulations of 2-amino-4-nitrophenol (**7**). As shown in Scheme 4, treatment of **7** with methyl 2,3-dibromopropanoate gave methyl 6-nitro-3,4-dihydro-2*H*-1,4-benzoxazine-2-carboxylate **8**, which was sequentially treated with $NaBH_4$ and methane sulfonyl chloride to give mesylate **9**. Displacement of the mesylate with various amines afforded the nitro compounds **42a**−**49a**. The amino derivatives **42b**−**49b** obtained by reduction of the nitro compounds with hydrogen in the presence of Pd/C were then treated with **3b** to afford the analogues **42** and **45**−**49**. The synthesis of the nitro intermediates **42a**−**45a** and the corresponding amines **42b**−**45b** have been disclosed.[9] Intermediate **9** was also treated with alkyl/aryl sulfonyl chloride to afford the *N*-sulfonyl aryl/methyl intermediates. Displacement of the mesylate with dimethylamine, reduction with hydrogen in the presence of Pd/C, and cyclization with **3b** afforded compounds **43** and **44**. The synthesis of the dihydrobenzodioxin analogues **50**−**54** involved similar transformations starting from 3,4-dihydroxynitrobenzene **10** and is represented by the synthesis of the *S*-antipode, as shown in Scheme 5. Monoprotection of the phenol with MOMCl, followed by treatment with (*R*)-glycidol in the presence of ditertbutyl azidocarboxylate gave the epoxide **11**. Deprotection of the MOM protecting group with HCl, followed by cyclization of the phenolic hydroxyl onto the epoxide, gave [(2*R*)-6-nitro-2,3-dihydro-1,4-benzodioxin-2-yl]methanol **12**. Conversion of the hydroxyl group in **12** to the mesylate using methane sulfonyl chloride, followed by its displacement with dimethylamine and subsequent reduction of the nitro group gave the amine **13**. Treatment of the amine **13** with **3b** afforded analogues **51** and **53**.

Table 2. Inhibitory Potencies (IC_{50}) vs hMCHR1[a]

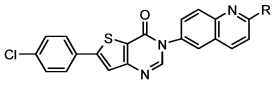

Cmpd	Structure (R)	IC_{50} (nM)	Cmpd	Structure (R)	IC_{50} (nM)
25	H	63	**34**	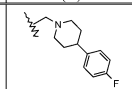	3.1
26		0.74	**35**	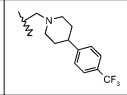	6.1
27		87	**36**	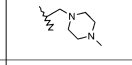	3.1
28		2.0	**37**	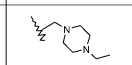	6.2
29		1.0	**38**	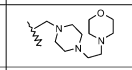	19
30		0.89	**39**	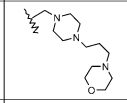	37
31		5.6	**40**	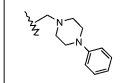	3.8
32		1.5	**41**	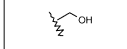	3.5
33		1.3			

[a] Antagonism of human MCHR1 in CHO Gal4/Elk1-Luc$^+$ reporter assay. IC_{50} values represent averages of 2−3 experiments, with a standard deviation of 3-fold.

Scheme 3. Synthetic Route to Targets **41**[a]

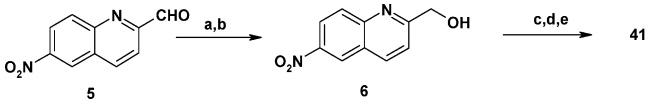

[a] Reagents and conditions: (a) $NaBH_4$, dioxane; (b) TBDMSCl, CH_2Cl_2, imidazole; (c) 10% Pd/C, H_2, 1 atm, 4 h; (d) **3b**, PhOH, 100−135 °C; (e) TBAF, THF.

Results and Discussion

In the process of optimizing the 6-position of the thieno[3,2-*d*]pyrimidinone core, analogues **14**−**24** were synthesized. The

Scheme 4. Synthetic Route to Targets **42**−**49**[a]

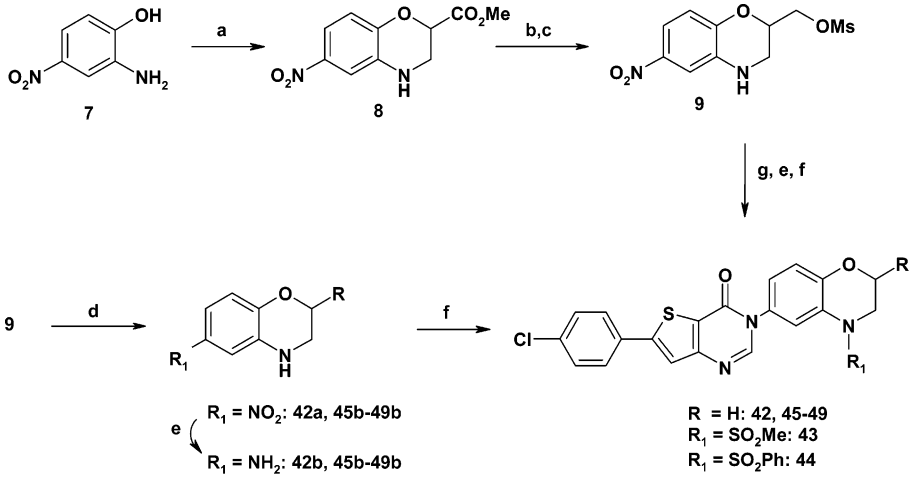

[a] Reagents and conditions: (a) methyl 2,3-dibromopropanoate; (b) $NaBH_4$, MeOH; (c) CH_3SO_2Cl, CH_2Cl_2, Hunig's base; (d) dialkylamine, CH_2Cl_2, Hunig's base; (e) 10% Pd/C,H_2, 30 psi; (f) **3b**, PhOH, 100−135 °C; (g) alkyl/aryl sulfonyl chloride, Hunig's base, CH_2Cl_2.

Scheme 5. Synthetic Route to Targets **51** and **53**[a]

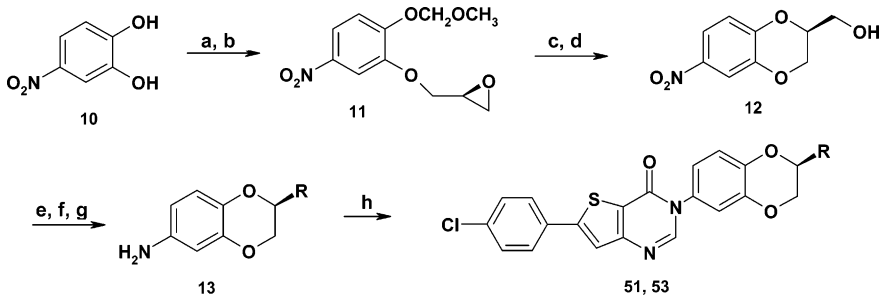

[a] Reagents and conditions: (a) MOMCl, K_2CO_3, DMF; (b) (*R*)-glycidol, di-tertbutyl azidocarboxylate, CH_2Cl_2; (c) HCl; (d) K_2CO_3, MeOH; (e) CH_3SO_2Cl, CH_2Cl_2, Hunig's base; (f) dialkylamine, CH_2Cl_2, Hunig's base; (g) 10% Pd/C, H_2, 30 psi; (h) **3b**, PhOH, 100−135 °C.

unsubstituted phenyl analogue **14** (IC_{50} = 794 nM) was a modest inhibitor of MCH in the reporter gene assay. Addition of halogens at the 2-, 3-, and 4-position on the phenyl resulted in analogues **15**−**19**. The 4-chloro as well as the 4-bromo analogues **15** (IC_{50} = 4.9 nM) and **18** (IC_{50} = 40 nM), respectively, were among the most potent compounds that resulted from halogen substitutions. Having established the 4-position to be potency enhancing, the effects of other electron-withdrawing and electron-donating groups were also studied. The cyano analogue **20** (IC_{50} = 478 nM) resulted in a 97-fold loss in activity compared to **15**, whereas the trifluoromethyl analogue **21** (IC_{50} = 36 nM) and the methoxy analogue **22** (IC_{50} = 31 nM) suffered a modest loss in potency (vs **15**). To probe the steric requirements in the 4-position, compounds **23** and **24** were synthesized; these resulted in substantial loss in activity. Interestingly, even a slightly bigger halogen substitution such as in the 4-bromo analogue **18** resulted in an 8-fold loss in potency when compared to **15**.

With the 4-chlorophenyl substituent in place at the 6-position of the thieno[3,2-*d*]pyrimidin core, modifications at the ortho-position of the quinoline nitrogen were studied with the aim of optimizing the potency and physiochemical properties of the molecules. As shown in Table 2, removal of the side chain morpholino group from analogue **15** afforded compound **25** (IC_{50} = 63 nM), which was 12-fold less active than analogue **15**. Because the basic nitrogen seemed to boost the activity, various analogues containing a basic amine differing in pK_a values were incorporated (**26**−**40**).[10] Simple alkylamine substitutions on the quinoline such as in analogues **26** and **29**−**32**, having pK_a values in the range of 7.17−7.37, were found to be 3.2−6.6-fold more active than the morpholino analogue **15** (pK_a = 5.26). Incorporation of a 4-fluoro or 4-trifluoromethyl group on the phenyl piperidine analogue **33**, to address the potential site of metabolism at the 4-position, afforded analogues **34** (IC_{50} = 3.1 nM) and **35** (IC_{50} = 6.1 nM), which were equipotent to analogue **15**. The piperidine analogue **30** (pK_a = 4.80, nitrogen proximal to quinoline moiety) was found to be equipotent to analogue **15**. Attenuation of the basicity of the nitrogen, as in analogues **27** (IC_{50} = 87 nM, pK_a = 1.59), resulted in a 17-fold drop in potency. On the other hand, incorporation of the nitrogen as in the imidazole analogue **28** (IC_{50} = 2.0, pK_a = 6.19) did not have any apparent effect on the potency. Incorporation of an additional nitrogen in the piperidine analogue **30** afforded the piperazines **36**−**40**. Analogues **36**, **37**, and **40** were equipotent to analogue **15**, whereas analogues **38** (IC_{50} = 19 nM) and **39** (IC_{50} = 37 nM) suffered a 3.9- and 7.5-fold drop in potency, respectively. Replacement of the basic nitrogen with a hydroxyl group resulted in analogue **41** (IC_{50} = 3.5 nM, pK_a = 13.14), which was equipotent in activity to **15**. Analysis of the calculated pK_a values suggests that, in general, with the exception of analogues **38** and **39**, analogues that possessed sterically demanding basic substituents, and analogue **41**, containing a neutral hydroxyl, there was a good correlation of the pK_as with the activity of the compounds, suggesting the possibility of either a charged interaction or a hydrogen bonding interaction with the receptor. The enhanced potency of analogue **41** could be due to the presence of a hydrogen bonding interaction with the receptor. In addition, the presence of the quinoline nitrogen in analogue **41** makes the hydroxyl a better hydrogen bond donor. Furthermore, in analogues **26** and **29**−

Table 3. Inhibitory Potencies (IC_{50}) vs hMCHR1[a]

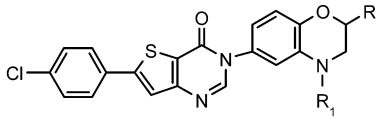

Cmpd	Structure (R)	(R_1)	IC_{50} (nM)	Cmpd	Structure (R)	(R_1)	IC_{50} (nM)
42		H	3.2	**46**	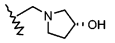	H	3.4
43		SO_2Me	4168	**47**	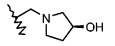	H	5.3
44		SO_2Ph	6918	**48**	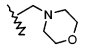	H	8.5
45		H	2.3	**49**	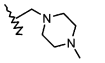	H	3.5

[a] Antagonism of human MCHR1 in CHO Gal4/Elk1-Luc$^+$ reporter assay. IC_{50} values represent averages of 2−3 experiments, with a standard deviation of 3-fold.

Table 4. Inhibitory Potencies (IC_{50}) vs hMCHR1[a]

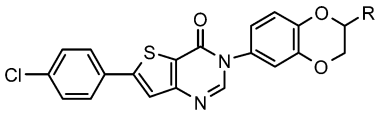

Cmpd	Structure (R)	IC_{50} (nM)	Cmpd	Structure (R)	IC_{50} (nM)
50		7.7	**53**		24
51		25	**54**		7.0
52		3.2			

[a] Antagonism of human MCHR1 in CHO Gal4/Elk1-Luc$^+$ reporter assay. IC_{50} values represent averages of 2−3 experiments, with a standard deviation of 3-fold.

32 (pK_as ranging from 7.17 to 7.37), with charges associated with their basic nitrogen and the percentage ionized ranging from 37 to 52%, a reduction in pK_a such as in example **27** (pK_a = 1.59) results in a large percent decrease in the percentage ionized and a concomitant loss in activity. Interestingly, at physiological pH, analogue **28** (pK_a = 6.19) with about 6.8% ionized molecules is apparently equipotent to analogue **15** (pK_a = 5.81, 0.71% ionized).

Having explored the quinoline analogues, attempts to address the solubility of these compounds resulted in analogues **42**−**49** (Table 3). In general, the 3,4-dihydro-1,4-benzoxazine derivatives had comparable potencies to analogue **15**. Addition of electron-withdrawing substituents on the NH group as in analogues **43** (IC_{50} = 4168 nM) and **44** (IC_{50} = 6918 nM) resulted in a dramatic loss in potency. In the hydroxy proline analogues **46** and **47**, the stereochemistry of the hydroxyl group in the proline derivatives **46** (IC_{50} = 3.4 nM) and **47** (IC_{50} = 5.3 nM) did not seem to effect the potency of the compounds. Replacement of the NH in the benzoxazine core with oxygen gave 2,3-dihydro-1,4-benzodioxin analogues **50**−**54** (Table 4**)**. In general, the benzodioxin analogues also had comparable potency to analogue **15**. To address stereochemical issues in the benzodioxin series, the *R*- as well as *S*-antipodes of analogue **50** were synthesized. The *S*-antipodes **51** and **53** were found to be 3.4- to 7.8-fold less active, respectively, than the *R*-antipodes, indicating the importance of an optimal spatial arrangement of the basic amine in its interaction with the receptor.

Homology Modeling

The initial homology model for MCHR1 was constructed for the 11CBy short splice variant, and the sequence numbering is based on this form. The template for the homology model was the published crystal structure for bovine rhodopsin. The models were constructed using the Modeler tools in Insight from Accelrys. Four different versions of this initial model were prepared by rotating selected side chains on internal residues in the transmembrane helices. Analogue **30** was docked into these models using the mcdock and dockmin applications in the Flo software package (flo+apr2003).

A number of docking poses were obtained for each of the starting receptor models. Compound **30**, a more rigid MCH ligand, is a good structure for evaluating the possible docking poses. Visual inspection of the docking results showed that the docking pose exemplified in Figure 1 was favored. In this pose, the piperidinium group forms an ionic and hydrogen bond to Asp123, and the pyrimidine ring carbonyl is hydrogen bonded by Tyr273. Figure 2 shows the details of the chlorophenyl binding pocket. This group is tightly packed amid Thr131 and Leu134 on TM3 and Pro220 and Ile224 on TM5. As seen from the tight SAR of analogues **18**, **23**, and **24** in Table 1, and modeling studies, very little room is available in this pocket for substitutions that are sterically demanding. Figure 3 shows the details of the piperidinium binding pocket. This pocket is formed from hydrophobic groups from TM1, 2, 6, and 7 and ECL2 and Asp123 from TM3. This model shows room for small substituents at C-2 and C-3, but limited room at C-4 on the piperidine ring, which is consistent with the lower potency of compounds such as **38** and **39** substituted at that position. Compounds with large substituents on the basic amine may suffer unfavorable steric interactions, which result in a loss in potency when compared to compound **30**, despite otherwise favorable interactions. In addition, the SAR done in this region of the molecule suggests the presence of a charged or hydrogen bonding interaction. This conclusion is supported by our modeling studies that propose a direct interaction of the protonated amine with Asp123. This model also explains the enhanced potency of analogue **41**, wherein a favorable hydrogen binding interaction of the hydroxyl with Asp123 can substitute for the absence of a charged basic amine. Although the hydroxyl interaction with Asp123 might not be as strong as opposed to that with a basic amine that is physiologically charged, there is

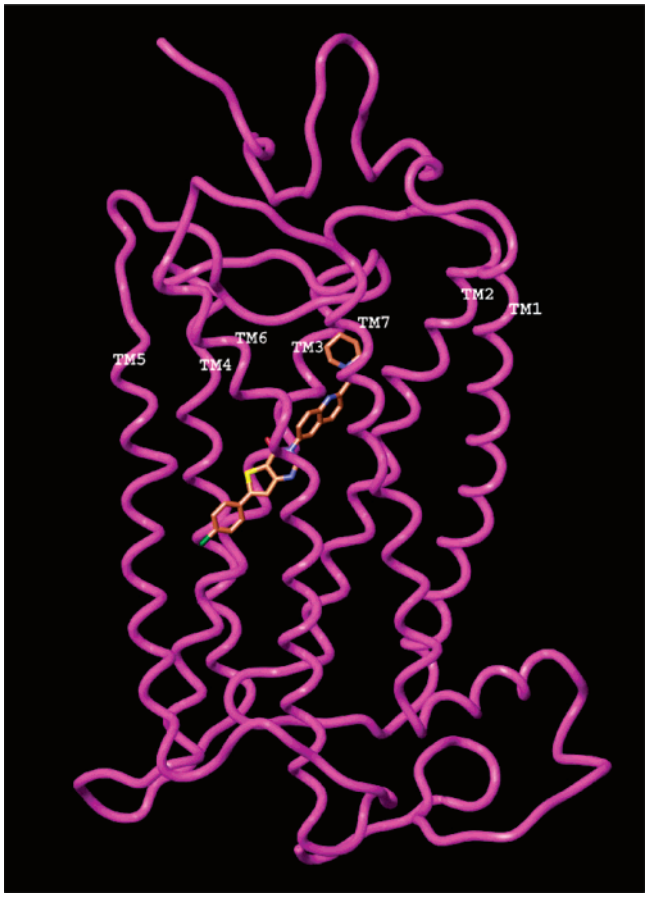

Figure 1. Binding mode for compound **30**. The preferred binding mode is in the top half of the helices, primarily between TM3, TM5, TM6, and TM7, with the axis of the compound approximately parallel to TM3.

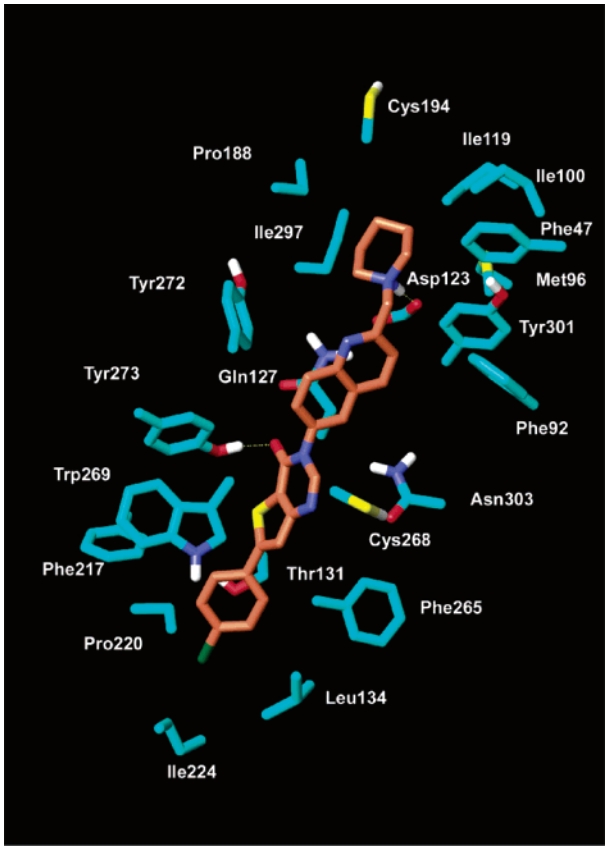

Figure 2. Binding interactions of compound **30**. This figure shows residues within 3 Å of the compound. This binding mode shows hydrogen bonds to Asp123 and from Tyr273. The pockets around the ends of the molecule are hydrophobic, while the central region is more polar.

a desolvation penalty that the hydroxyl group does not have to overcome, so the two fragments might have similar binding energies due to cancellation of effects. Our proposed binding mode differs from that proposed by Clark for a somewhat more flexible ligand.[5i] Although the basic amine in compound **30** binds in a similar position to that proposed by Clark, the remainder of the molecule lies parallel to the axis of TM3 and probes deeper into the receptor. If the quinoline of **30** were placed in a position similar to that of Clark's compound, the chlorophenyl group would protrude from the side of the receptor. Finding alternative binding modes for different chemotypes is not unusual among antagonists.

Pharmacokinetic Analysis and Secondary Pharmacology

To evaluate compounds in an in vivo model of DIO mice, representative compounds were profiled for pharmacokinetic properties in rats. As seen in Table 5, analogue **33** when dosed as a solution exhibited decent oral bioavailability of 19% with low clearance (11 mL/min/kg) and a good half-life ($t_{1/2} = 8$ h). Incorporation of a fluoro or trifluoromethyl group at the 4-position of the phenylpiperazine in analogue **33** to block potential metabolism afforded analogues **34** and **35** with 3.7-fold and 2.9-fold lower clearances, respectively, and an extremely long half-life for analogue **34** ($t_{1/2} = 16$ h), with analogue **34** affording a slightly better systemic exposure on oral dosing when compared to analogue **33**. The *N*-methylpiperazine analogue **36** was found to have excellent systemic exposure, with a bioavailability of 98% and quite a good half-life ($t_{1/2} = 7.7$ h). The clearance of analogue **36** (39.7 mL/min/Kg) was on the higher side, possibly due to *N*-demethylation of the piperazine ring. A few of the analogues incorporating additional heteroatoms to increase their solubility were also profiled as shown in Table 5. The dimethyl analogue **42** had extremely high clearance (88 mL/min/kg), exceeding the hepatic blood flow in rats. To prevent potential *N*-demethylation and/or conjugation of the NH in analogue **42**, the benzodioxane analogue **54** was synthesized. Unfortunately, although this change did result in improved systemic exposure, the clearance of this analogue was still extremely high (66 mL/min/kg). Because analogue **36** had good solubility and extremely good oral exposure, compound **36** was profiled against a battery of 7TM receptors, enzymes, and ion channels, and no significant off-target activity was observed for compound **36**. In addition, the compound showed no activity in the hERG channel using the patch clamp assay ($pIC_{50} = 4.66$).[11] It was also selective over the human MCHR2.

Pharmacodynamics

Efficacy of compound **36** in inducing weight loss was evaluated in high-fat (58% kcal of fat, Research Diets #D12331), DIO AKR/J mice. As shown in Figure 4, during a 26-day treatment, oral administration of compound **36** at 1, 3, and 10 mg/kg once daily caused a sustained dose-dependent weight loss of −4.8, −9.4, and −16.9%, respectively, relative to vehicle controls. Analysis of terminal serum and brain concentrations of compound **36** levels revealed that the compound is absorbed into the circulation (44 ± 2.7 ng/mL, 178 ± 12.6 ng/mL, and 414 ± 17.1 ng/mL at 1, 3, and 10 mg/kg, respectively) and it penetrates the brain (1421 ± 70.5 ng/g, 5508 ± 162 ng/g, and

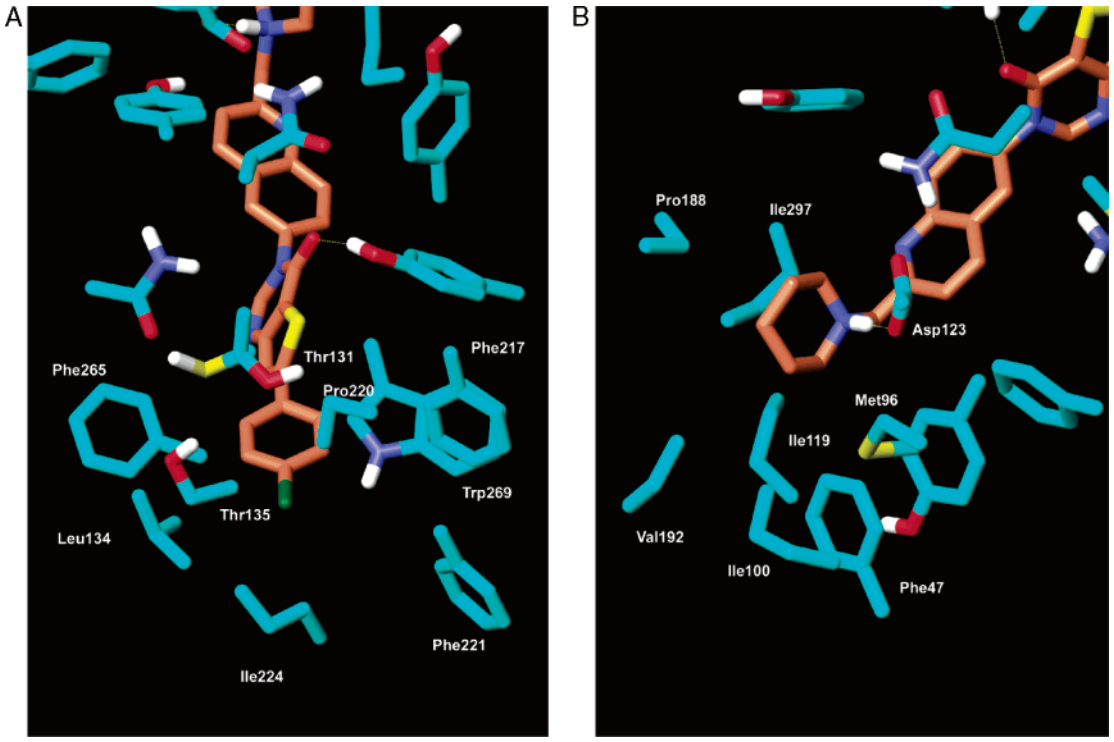

Figure 3. Details of Binding Pockets. (A) The chlorophenyl ring is tightly packed in a hydrophobic pocket formed by Thr131, Leu134, Thr135, Phe217, Pro220, Phe221, Ile224, Phe265, and Trp269. (B) The piperidine pocket in addition to Asp123 includes the hydrophobic groups Met96, Phe47, Ile100, Ile119, Val192, Pro188, and Ile297.

Table 5. Rat Pharmacokinetic Data for Representative Analogues[a]

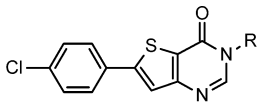

Cmpd	R	Cl_{total} (mL/min/kg)	V_{ss} (L/kg)	$t_{1/2}$ (h)[b]	F (%)
33	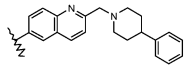	11	4.3	8	19
34	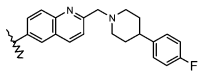	2.9	2.3	16	30
35	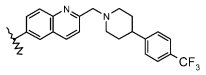	3.7	1.1	8.5	18
36	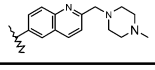	39	19	7.7	98
42	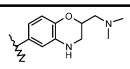	88	27	8	75
53	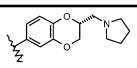	66	22	6.1	65

[a] Compounds were dosed in 20% DMSO/21% Solutol in 10 mM (final conc) MSA ($n = 2$); IV dosing done at 3 mg/kg and PO dosing done at 10 mg/kg. [b] Half-life for IV dosing; plasma drug levels were determined by LC-MS/MS.

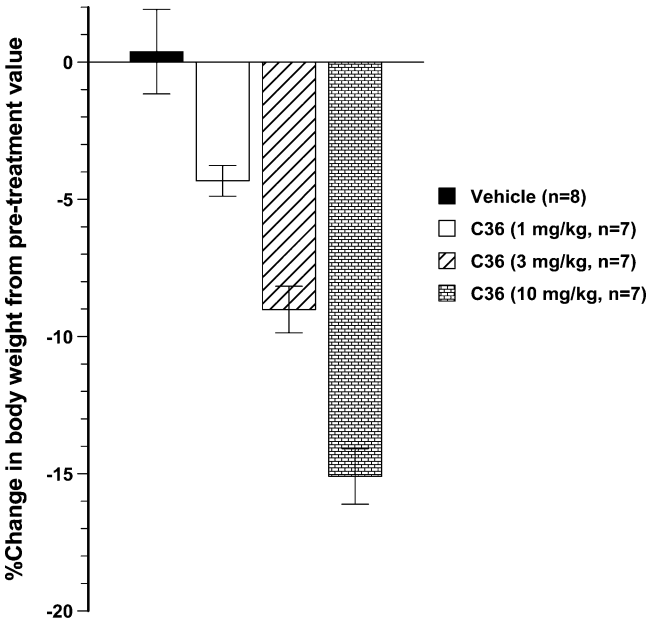

Figure 4. Effect of compound **36** (**C36**) at 1, 3, and 10 mg/kg (orally, qd) on body weight loss in high-fat DIO AKR/J mice. Weight loss is expressed as percentage weight change from pretreatment value for each treatment group (average pretreatment body weight value was 48.8 ± 0.61 g, $n = 21$). Values are mean ± SEM, n = number of mice per group.

13093 ± 392 ng/g at 1, 3, and 10 mg/kg, respectively) at all doses with a relatively stable brain/serum ratio of 31.

Conclusion

Structure−activity work on the thienopyrimidinone core has resulted in the identification of potent and selective MCHR1 antagonists. Homology modeling of these compounds indicate the importance of Asp123 as a key element in the protein that helps provide added potency with compounds that have favorable binding counterparts. Several compounds in the series also exhibited favorable pharmacokinetic properties on oral dosing in rats. A representative analogue, when dosed orally once daily to DIO AKR mice, exhibited a very good dose responsive effect in reducing body weight. This work supports the advancement

of small molecule MCHR1 antagonist into human clinical trials for the treatment of obesity.

Experimental Section

Chemistry. General Methods. Melting points were determined using a Thomas−Hoover melting point apparatus and are uncorrected. Unless stated otherwise, reagents were obtained from commercial sources and were used directly. Reactions involving air- or moisture-sensitive reagents were carried out under a nitrogen atmosphere. If not specified, reactions were carried out at ambient temperature. Silica gel (EM Science, 230−400 mesh) was used for chromatographic purification unless otherwise indicated. Anhydrous solvents were obtained from Aldrich (Sure Seal). ^{1}H NMR spectra were recorded on a Varian spectrometer; chemical shifts are reported in parts per million (ppm) relative to TMS. The following abbreviations are used to describe peak patterns when appropriate: b = broad, s = singlet, d = doublet, t = triplet, q = quartet, m = multiplet. High performance liquid chromatography (HPLC) was performed on a Beckman 126 with a Beckman 166 UV Detector (monitoring at 215 nm) with a Rainin Dynamax-60A column using a gradient consisting of 20/80 A/B to 10/90 A/B over 20 min, where A = 1% aqueous trifluoroacetic acid (TFA) and B = 1% TFA in CH_3CN. Elemental analyses, performed by Atlantic Microlab, Inc., Norcross, GA, were within 0.4% of the theoretical values calculated for C, H, and N. For compounds that did not have elemental analysis purity were determined by using two different methods. Method A, MeOH/H_2O from 0 to 100%; method B, CH_3CN/H_2O from 10 to 100%. Compounds were found to be >95% in purity by both methods A and B unless otherwise as stated in the experimental.

General Procedure for the Synthesis of Amidenes 3a−3k: Methyl-3-{[(1*E*)−(dimethylamino)methylidene]amino}-5-phenyl-2-thiophenecarboxylate (3a). A mixture of methyl 3-amino-5-(phenyl)-2-thiophenecarboxylate (10.0 g, 42.9 mmol) and *N*,*N*-dimethylformamide dimethyl acetal (8.9 g, 74.7 mmol) was heated at 95 °C for 3 h. The solvent was removed by rotary evaporation. To the residue ether was added, and the reaction was left in the freezer for 16 h. The resulting solid was collected by filtration giving the desired product in quantitative yield. ^{1}H NMR (300 MHz, DMSO-d_6): δ 7.89 (s, 1H), 7.74−7.38 (m, 5H), 7.33 (s, 1H), 3.73 (s, 3H), 3.06 (s, 3H), 2.99 (s, 3H).

General Procedure for the Synthesis of Nitro Compounds 14a, 26a−39a, and 45a−48a: 2-(Morpholin-4-ylmethyl)-6-nitroquinoline (14a): 2-(Bromomethyl)-6-nitroquinoline. To a solution of 2-methyl-6-nitroquinoline (10.0 g, 53.2 mmol) and *N*-bromosuccinimide (20.0 g, 111.72 mmol) in 120 mL of acetonitrile was added AIBN (0.7 g), and the contents were heated at 70 °C for 16 h to afford a mixture of monobromo (57%) and dibromo (43%) compounds. After cooling the crude reaction mixture to 20 °C, diethyl phosphate (3.97 mL, 28.7 mmol) was added, followed by the addition of triethylamine (4.29 mL, 30.8 mmol). After stirring for 30 min, water (60 mL) and 1 N NaOH (25 mL) was added, and then the contents were stirred for an additional 10 min. The precipitated brown solid was filtered, washed with water, and dried under vacuum to afford 2-(bromomethyl)-6-nitroquinoline as a pale yellow solid (7.78 g, 55%). ^{1}H NMR (300 MHz, DMSO-d_6): δ 9.10 (s, 1H), 8.78 (d, J = 8.6 Hz, 1H), 8.52 (d, J = 9.8 Hz, 1H), 8.23 (d, J = 9.2 Hz, 1H), 7.92 (d, J = 8.5 Hz, 1H), 4.93 (s, 2H). ES-LCMS *m*/*z*: 267 (M + H).

2-(Morpholin-4-ylmethyl)-6-nitroquinoline (14a). To a solution of 2-(bromomethyl)-6-nitroquinoline (1.0 g, 3.76 mmol) in THF at room temperature was added Hunig's base (1.31 mL, 7.52 mmol), followed by the addition of morpholine (0.327 g, 3.76 mmol). The contents were stirred for 3 h at room temperature. The crude reaction mixture was concentrated and loaded directly over a silica gel column using hexane/ethyl acetate 1:1 as the eluent to afford 6-2-(morpholin-4-ylmethyl)-6-nitroquinoline as a brown solid (1.05 g, 81%). ^{1}H NMR (300 MHz, DMSO-d_6): δ 9.08 (s, 1H), 8.72 (d, J = 8.6 Hz, 1H), 8.48 (d, J = 9.1 Hz, 1H), 8.21 (d, J = 9.2 Hz, 1H), 7.89 (d, J = 8.6 Hz, 1H), 3.89 (s, 2H), 3.66 (m, 4H), 2.54 (m, 4H).

General Procedure for the Synthesis of Amino Compounds 14b, 27b−39b, and 45b−48b 2-(Morpholin-4-ylmethyl)quinolin-6-amine (14b). To a solution of 2-(morpholin-4-ylmethyl)-6-nitroquinoline **15a** (1.0 g, 2.88 mmol) in 30 mL THF/EtOH (1:1) was added 0.1 g of Pd/C (10%), and the contents were stirred under hydrogen gas (40 psi) for 6 h. The reaction was then filtered through Celite and washed with EtOH, and the contents were concentrated under vacuum to afford 2-(morpholin-4-ylmethyl)quinolin-6-amine as a brown solid. The crude compound was used directly in the next step. ^{1}H NMR (300 MHz, DMSO-d_6): δ 7.93 (d, J = 8.6 Hz, 1H), 7.69 (d, J = 9.0 Hz, 1H), 7.41 (d, J = 8.5 Hz, 1H), 7.21−7.11 (m, 1H), 6.81 (m, 1H), 5.55 (s, 2H), 3.65 (s, 2H), 3.61 (m, 4H), 2.51 (m, 4H).

General Procedure for the Synthesis of Final Products 14−52: 3-[2-(4-Morpholinylmethyl)-6-quinolinyl]-6-phenylthieno-[3,2-*d*]pyrimidin-4(3*H*)-one (14). To 2-(morpholin-4-ylmethyl)-quinolin-6-amine **14b** (0.123 g, 0.506 mmol) was added methyl-3-{[(1*E*)-(dimethylamino)methylidene]amino}-5-phenyl-2-thiophenecarboxylate (0.145 g, 0.506 mmol) and 0.5 g of phenol as the solvent. The reaction mixture was heated from 100 to 135 °C over a period of 1.5 h. The crude mixture was loaded over a silica gel column using DCM/MeOH (95:5) to afford 6-(4-chlorophenyl)-3-[2-(morpholin-4-ylmethyl)quinolin-6-yl]thieno[3,2-d]pyrimidin-4(3*H*)-one as a yellow solid (0.101 g, 44%). ^{1}H NMR (300 MHz, DMSO-d_6): δ 8.57 (s, 1H), 8.42 (d, J = 8.6 Hz, 1H), 8.19 (s, 1H), 8.12 (d, J = 9.0 Hz, 1H), 8.01 (s, 1H), 7.95−7.90 (m, 3H), 7.75 (d, J = 8.4 Hz, 1H), 7.59 (m, 2H), 3.79 (s, 2H), 3.61 (m, 4H), 2.48 (m, 4H). Elemental analysis was performed for C, H, and N.

6-(4-Chlorophenyl)-3-[2-(4-morpholinylmethyl)-6-quinolinyl]-thieno[3,2-*d*]pyrimidin-4(3*H*)-one (15). ^{1}H NMR (300 MHz, DMSO-d_6): δ 8.57 (s, 1H), 8.42 (d, J = 8.6 Hz, 1H), 8.19 (s, 1H), 8.12 (d, J = 9.0 Hz, 1H), 8.01 (s, 1H), 7.95−7.90 (m, 3H), 7.75 (d, J = 8.4 Hz, 1H), 7.59 (m, 2H), 3.79 (s, 2H), 3.61 (m, 4H), 2.48 (m, 4H). Elemental analysis was performed for C, H, and N.

6-(3-Chlorophenyl)-3-[2-(4-morpholinylmethyl)-6-quinolinyl]-thieno[3,2-*d*]pyrimidin-4(3*H*)-one (16). ^{1}H NMR (300 MHz, DMSO-d_6): δ 8.62 (s, 1H), 8.47 (d, J = 8.6 Hz, 1H), 8.24 (s, 1H), 8.17−8.07 (m, 4H), 7.96−7.86 (m, 2H), 7.80 (d, J = 8.4 Hz,1H), 7.59 (s, 1H), 3.84 (s, 2H), 3.65 (m, 2H), 2.53 (m, 2H). Purity was determined using methods A and B.

6-(2-Chlorophenyl)-3-[2-(4-morpholinylmethyl)-6-quinolinyl]-thieno[3,2-*d*]pyrimidin-4(3*H*)-one (17). ^{1}H NMR (300 MHz, DMSO-d_6): δ 8.62 (s, 1H), 8.47 (d, J = 8.6 Hz, 1H), 8.24 (s, 1H), 8.19−8.13 (m, 4H), 7.96−7.86 (m, 2H), 7.80 (d, J = 8.4 Hz, 1H), 7.59 (s, 1H), 3.84 (s, 2H), 3.65 (m, 2H), 2.53 (m, 2H). Elemental analysis was performed for C, H, and N.

6-(4-Bromophenyl)-3-[2-(4-morpholinylmethyl)-6-quinolinyl]-thieno[3,2-*d*]pyrimidin-4(3*H*)-one (18). ^{1}H NMR (300 MHz, DMSO-d_6): δ 8.62 (s, 1H), 8.47 (d, J = 8.6 Hz, 1H), 8.24 (s, 1H), 8.17 (d, J = 8.9 Hz, 1H), 8.07 (s, 1H), 7.96−7.90 (m, 3H), 7.80−7.75 (m, 3H), 3.84 (s, 2H), 3.66 (m, 2H), 2.54 (m, 2H). Elemental analysis was performed for C, H, and N.

6-(4-Fluorophenyl)-3-[2-(4-morpholinylmethyl)-6-quinolinyl]-thieno[3,2-*d*]pyrimidin-4(3*H*)-one (19). ^{1}H NMR (300 MHz, DMSO-d_6): δ 8.61 (s, 1H), 8.47 (d, J = 8.5 Hz, 1H), 8.24 (s, 1H), 8.17 (d, J = 8.9 Hz, 1H), 8.02−7.92 (m, 4H), 7.80 (d, J = 8.5 Hz, 1H), 7.63−7.38 (m, 2H), 3.85 (s, 2H), 3.64 (m, 2H), 2.55 (m, 2H). Purity was determined using method B.

6-(4-Cyanol)-3-[2-(4-morpholinylmethyl)-6-quinolinyl]thieno-[3,2-*d*]pyrimidin-4(3*H*)-one (20). ^{1}H NMR (300 MHz, DMSO-d_6): δ 8.61 (s, 1H), 8.45 (d, J = 8.5 Hz, 1H), 8.34 (s, 1H), 8.17 (d, J = 8.9 Hz, 1H), 8.02−7.92 (m, 4H), 7.80 (d, J = 8.5 Hz, 1H), 7.63−7.38 (m, 2H), 3.85 (s, 2H), 3.64 (m, 2H), 2.55 (m, 2H). Elemental analysis was performed for C, H, and N.

3-[2-(4-Morpholinylmethyl)-6-quinolinyl]-6-[4-(trifluoromethyl)phenyl]thieno[3,2-*d*]pyrimidin-4(3*H*)-one (21). ^{1}H NMR (300 MHz, DMSO-d_6): δ 8.66 (m, 2H), 8.37 (s, 1H), 8.29 (d, J = 9.0 Hz, 1H), 8.21−8.08 (m, 3H), 8.06 (d, J = 8.4 Hz, 1H), 7.94−7.86 (m, 3H), 3.95 (s, 2H), 3.67 (m, 2H), 2.55 (m, 2H). Purity was determined using methods A and B.

6-[4-(Methyloxy)phenyl]-3-[2-(4-morpholinylmethyl)-6-quinolinyl]thieno[3,2-*d*]pyrimidin-4(3*H*)-one (22). ^{1}H NMR (300 MHz, DMSO-d_6): δ 8.62 (s, 1H), 8.47 (d, J = 8.5 Hz, 1H), 8.24 (s, 1H), 8.17 (d, J = 8.9 Hz, 1H), 8.13−8.07 (m, 3H), 7.96−7.90 (m, 2H), 7.80 (d, J = 8.5 Hz, 1H), 7.59 (m, 2H), 3.84 (s, 2H), 3.65 (m, 2H), 2.53 (m, 2H). Elemental analysis was performed for C, H, and N.

6-[4-(1-Methylpropyl)phenyl]-3-[2-(4-morpholinylmethyl)-6-quinolinyl]thieno[3,2-*d*]pyrimidin-4(3*H*)-one (23). ^{1}H NMR (300 MHz, DMSO-d_6): δ 8.59 (s, 1H), 8.46 (d, J = 8.5 Hz, 1H), 8.23 (s, 1H), 8.16 (d, J = 8.9 Hz, 1H), 7.95−7.76 (m, 5H), 7.20 (m, 2H), 3.84 (s, 2H), 3.65 (m, 2H), 2.53 (m, 2H). Elemental analysis was performed for C, H, and N.

6-[4-(1,1-Dimethylethyl)phenyl]-3-[2-(4-morpholinylmethyl)-6-quinolinyl]thieno[3,2-*d*]pyrimidin-4(3*H*)-one (24). ^{1}H NMR (300 MHz, DMSO-d_6): δ 8.60 (s, 1H), 8.47 (d, J = 8.5 Hz, 1H), 8.24 (s, 1H), 8.17 (d, J = 8.9 Hz, 1H), 7.96−7.77 (m, 6H), 7.59 (d, J = 8.5 Hz, 1H), 3.84 (s, 2H), 3.66 (m, 2H), 2.54 (m, 2H). Elemental analysis was performed for C, H, and N.

6-(4-Chlorophenyl)-3-(6-quinolinyl)thieno[3,2-*d*]pyrimidin-4(3*H*)-one (25). ^{1}H NMR (400 MHz, $CDCl_3$): δ 9.01 (s, 1H), 8.59 (s, 1H), 8.47 (d, J = 8.0 Hz, 1H), 8.23 (s, 1H), 8.18 (d, J = 8.9 Hz, 1H), 8.02 (s, 1H), 7.95 (d, J = 8.5 Hz, 1H), 7.66 (m, 1H), 7.59 (d, J = 8.5 Hz, 1H). Elemental analysis was performed for C, H, and N.

6-(4-Chlorophenyl)-3-{2-[(dimethylamino)methyl]-6-quinolinyl}thieno[3,2-*d*]pyrimidin-4(3*H*)-one (26). ^{1}H NMR (400 MHz, $CDCl_3$): δ 8.26 (d, J = 7.9 Hz, 1H), 8.25 (s, 1H), 8.21 (d, J = 8.2 Hz, 1H), 7.91 (d, J = 2.3 Hz, 1H), 7.76 (dd, J = 2.4 and 9.0 Hz, 1H), 7.72 (d, J = 8.4 Hz, 1H), 7.68 (d, J = 8.8 Hz, 2H), 7.57 (s, 1H), 7.46 (d, J = 8.8 Hz, 2H), 3.83 (s, 2H), 2.37 (s, 6H). EI-LCMS m/z: 447 (M + H).

6-(4-Chlorophenyl)-3-(2-{[methyl(phenyl)amino]methyl}-6-quinolinyl)thieno[3,2-*d*]pyrimidin-4(3*H*)-one (27). ^{1}H NMR (300 MHz, DMSO-d_6): δ 8.57 (s, 1H), 8.43 (d, J = 8.5 Hz, 1H), 8.39 (s, 1H), 8.31 (d, J = 9.0 Hz, 1H), 8.20 (s, 1H), 8.16 (m, 3H), 7.57 (m, 2H), 7.47 (d, J = 8.5 Hz, 1H), 7.15 (m, 2H), 6.77 (m, 2H), 6.62 (m, 1H), 4.87 (s, 2H), 3.17 (s, 3H).

6-(4-Chlorophenyl)-3-[2-(1*H*-imidazol-1-ylmethyl)-6-quinolinyl]thieno[3,2-*d*]pyrimidin-4(3*H*)-one (28). ^{1}H NMR (300 MHz, DMSO-d_6): δ 9.33 (s, 1H), 8.55 (m, 2H), 8.25 (s, 1H), 8.02 (s, 1H), 8.00 (s, 1H), 7.93 (m, 3H), 7.83 (s, 1H), 7.75 (s, 1H), 7.68 (d, J = 8.6 Hz, 1H), 7.58 (d, J = 8.6 Hz, 2H), 5.84 (s, 2H). Elemental analysis was performed for C, H, and N.

6-(4-Chlorophenyl)-3-[2-(1-pyrrolidinylmethyl)-6-quinolinyl]-thieno[3,2-*d*]pyrimidin-4(3*H*)-one (29). ^{1}H NMR (400 MHz, $CDCl_3$): δ 8.25−8.23 (m, 2H), 8.18 (d, J = 8.4 Hz, 1H), 7.88 (d, J = 2.4 Hz, 1H), 7.75−7.70 (m, 2H), 7.67 (d, J = 8.4 Hz, 2H), 7.56 (s, 1H), 7.45 (d, J = 8.8 Hz), 3.99(s, 2H), 2.63 (br s, 4H), 1.85−1.82 (m, 4H). ES-LCMS m/z: 473 (M + H).

6-(4-Chlorophenyl)-3-[2-(1-piperidinylmethyl)-6-quinolinyl]-thieno[3,2-*d*]pyrimidin-4(3*H*)-one (30). ^{1}H NMR (300 MHz, DMSO-d_6): δ 8.64 (s, 1H), 8.63 (d, J = 9.1 Hz, 1H), 8.36 (s, 1H), 8.28 (d, J = 9.0 Hz, 1H), 8.07 (m, 5H), 7.65 (m, 2H), 3.50 (s, 2H), 2.53 (m, 4H), 1.86−1.49 (m, 6H). Elemental analysis was performed for C, H, and N.

6-(4-chlorophenyl)-3-(2-{[4-(1-pyrrolidinyl)-1-piperidinyl]-methyl}-6-quinolinyl)thieno[3,2-*d*]pyrimidin-4(3*H*)-one (31). ^{1}H NMR (300 MHz, DMSO-d_6): δ 8.60 (s, 1H), 8.32 (s, 1H), 8.25 (d, J = 8.9 Hz, 1H), 8.04 (m, 2H), 7.94 (m, 2H), 7.87 (d, J = 8.6 Hz, 1H), 7.29 (m, 1H), 7.19 (m, 2H), 3.42 (s, 2H), 2.98 (m, 1H), 2.09−1.54 (m, 16H). Elemental analysis was performed for C, H, and N.

6-(4-Chlorophenyl)-3-[2-({4-[2-(1-pyrrolidinyl)ethyl]-1-piperidinyl}methyl)-6-quinolinyl]thieno[3,2-*d*]pyrimidin-4(3*H*)-one (32). ^{1}H NMR (300 MHz, DMSO-d_6): δ 8.59 (m, 2H), 8.31 (s, 1H), 8.22 (d, J = 8.9 Hz, 1H), 8.03−7.89 (m, 5H), 7.60 (m, 2H), 3.44 (s, 2H), 2.92 (m, 2H), 1.98 (m, 2H), 1.87−1.26 (m, 17H). Elemental analysis was performed for C, H, and N.

6-(4-Chlorophenyl)-3-{2-[(4-phenyl-1-piperidinyl)methyl]-6-quinolinyl}thieno[3,2-*d*]pyrimidin-4(3*H*)-one (33). ^{1}H NMR (300 MHz, DMSO-d_6): δ 8.61 (s, 1H), 8.59 (s, 1H), 8.32 (s, 1H), 8.25 (d, J = 9.0 Hz, 1H), 8.03−7.90 (m, 5H), 7.60 (d, J = 8.4 Hz, 1H), 7.35−7.21 (m, 6H), 4.76 (s, 2H), 3.61−3.49 (m, 2H), 3.28−3.15 (m, 2H), 2.87 (m, 1H), 2.22−1.96 (m, 4 H). Elemental analysis was performed for C, H, and N.

6-(4-Chlorophenyl)-3-(2-{[4-(4-fluorophenyl)-1-piperidinyl]-methyl}-6-quinolinyl)thieno[3,2-*d*]pyrimidin-4(3*H*)-one (34). ^{1}H NMR (300 MHz, DMSO-d_6): δ 8.66 (s, 1H), 8.36 (s, 1H), 8.29 (d, J = 9.0 Hz, 1H), 8.07−7.91 (m, 8H), 7.65 (d, J = 8.7 Hz, 1H), 7.33 (m, 1H), 7.17 (m, 2H), 3.87 (s, 2H), 3.04 (m, 3H), 2.80 (m, 2H), 2.26 (m, 2H), 1.84 (m, 2H). Elemental analysis was performed for C, H, and N.

6-(4-Chlorophenyl)-3-[2-({4-[4-(trifluoromethyl)phenyl]-1-piperidinyl}methyl)-6-quinolinyl]thieno[3,2-*d*]pyrimidin-4(3*H*)-one (35). ^{1}H NMR (300 MHz, DMSO-d_6): δ 8.62 (s, 1H), 8.48 (d, J = 8.6 Hz, 1H), 8.24 (s, 1H), 8.18 (d, J = 9.0 Hz, 1H), 8.11−7.81 (m, 8H), 7.83 (d, J = 8.6 Hz, 1H), 7.70−7.38 (m, 2H), 3.89 (s, 2H), 3.03 (m, 3H), 2.75 (m, 2H), 2.24 (m, 2H) 1.81 (m, 2H). Elemental analysis was performed for C, H, and N.

6-(4-Chlorophenyl)-3-{2-[(4-methyl-1-piperazinyl)methyl]-6-quinolinyl}thieno[3,2-*d*]pyrimidin-4(3*H*)-one (36). ^{1}H NMR (300 MHz, DMSO-d_6): δ 8.56 (s, 1H), 8.42 (d, J = 8.6 Hz, 1H), 8.19 (s, 1H), 8.11 (d, J = 9.0 Hz, 1H), 8.02 (s, 1H), 7.94−7.88 (m, 3H), 7.75 (d, J = 8.5 Hz, 1H), 7.59 (m, 2H), 3.82 (s, 2H), 2.64−2.37 (m, 11H). Elemental analysis was performed for C, H, and N.

6-(4-Chlorophenyl)-3-{2-[(4-ethyl-1-piperazinyl)methyl]-6-quinolinyl}thieno[3,2-*d*]pyrimidin-4(3*H*)-one (37). ^{1}H NMR (300 MHz, DMSO-d_6): δ 8.62 (s, 1H), 8.48 (d, J = 8.6 Hz, 1H), 8.25 (s, 1H), 8.17 (d, J = 8.8 Hz, 1H), 8.06 (s, 1H), 8.0 (d, J = 8.4 Hz, 2H), 7.95−7.92 (m, 1H), 7.78 (d, J = 8.5 Hz, 1H), 7.65 (d, J = 8.4 Hz, 2H), 3.87 (s, 2H), 2.76−2.53 (m, 9H), 1.03 (t, J = 7.2 Hz, 3H). Elemental analysis was performed for C, H, and N.

6-(4-Chlorophenyl)-3-[2-({4-[2-(4-morpholinyl)ethyl]-1-piperazinyl}methyl)-6-quinolinyl]thieno[3,2-*d*]pyrimidin-4(3*H*)-one (38). ^{1}H NMR (300 MHz, DMSO-d_6): δ 8.63 (s, 1H), 8.43 (d, J = 8.6 Hz, 1H), 8.27 (s, 1H), 8.17 (d, J = 9.1 Hz, 1H), 8.05 (s, 1H), 8.0 (d, J = 8.6 Hz, 2H), 7.94−7.90 (m, 1H), 7.78 (d, J = 8.6 Hz, 1H), 7.67 (d, J = 8.6 Hz, 2H), 3.81 (s, 2H), 3.61 (m, 4H), 2.58−2.11 (m, 16H). Elemental analysis was performed for C, H, and N.

6-(4-Chlorophenyl)-3-[2-({4-[3-(4-morpholinyl)propyl]-1-piperazinyl}methyl)-6-quinolinyl]thieno[3,2-*d*]pyrimidin-4(3*H*)-one (39). ^{1}H NMR (300 MHz, DMSO-d_6): δ 8.61 (s, 1H), 8.46 (d, J = 8.5 Hz, 1H), 8.24 (s, 1H), 8.16 (d, J = 9.0 Hz, 1H), 8.06 (s, 1H), 8.0 (d, J = 8.5 Hz, 2H), 7.95−7.91 (m, 1H), 7.77 (d, J = 8.5 Hz, 1H), 7.64 (d, J = 8.5 Hz, 2H), 3.83 (s, 2H), 3.60 (m, 4H), 2.60−2.10 (m, 16H), 1.63 (m, 2H). Elemental analysis was performed for C, H, and N.

6-(4-Chlorophenyl)-3-{2-[(4-phenyl-1-piperazinyl)methyl]-6-quinolinyl}thieno[3,2-*d*]pyrimidin-4(3*H*)-one (40). ^{1}H NMR (300 MHz, DMSO-d_6): δ 8.62 (s, 1H), 8.60 (s, 1H), 8.32 (s, 1H), 8.25 (d, J = 9.0 Hz, 1H), 8.03−7.94 (m, 4H), 7.84 (d, J = 8.4 Hz, 1H), 7.60 (m, 2H), 7.28 (m, 1H), 7.16 (m, 1H), 7.00 (d, J = 8.2 Hz, 1H), 6.87 (t, J = 7.2 Hz, 1H), 6.74 (d, J = 7.7 Hz, 1H), 4.84 (s, 2H), 3.54 (m, 4H), 2.07 (m, 4H). Elemental analysis was performed for C, H, and N.

6-(4-Chlorophenyl)-3-[2-(hydroxymethyl)-6-quinolinyl]thieno-[3,2-*d*]pyrimidin-4(3*H*)-one (41). (a) 6-Nitroquinoline-2-carbaldehyde. To a hot solution of selenium dioxide (41.6 g, 375 mmol) in dioxane (185 mL) and water (35 mL) was added 2-methyl-6-nitroquinoline (47.0 g, 250 mmol). The mixture was refluxed for 30 min. The selenium black was filtered off, and the filtrate was concentrated by rotary evaporation. The resulting solid was washed with a saturated solution of sodium bicarbonate. The solid was filtered, washed with water, and dried to give the product as a tan solid (44.8 g, 89%). ^{1}H NMR (300 MHz, DMSO-d_6): δ 10.17 (s, 1H), 9.21 (d, J = 2.6 Hz, 1H), 8.97 (d, J = 8.5 Hz, 1H), 8.59 (dd, J = 2.6 and 9.2 Hz, 1H), 8.44 (d, J = 9.2 Hz, 1H), 8.16 (d, J = 8.5 Hz, 1H).

(b) (6-Nitro-2-quinolinyl)methanol. To 6-nitro-2-quinolinecarbaldehyde (500 mg, 2.47 mmol) in a 50% mixture of ethyl alcohol and 1,4-dioxane (30 mL) at 0 °C was added sodium borohydride (188 mg, 4.95 mmol). After stirring for 10 min, the reaction mixture

was poured into ice-cold water and extracted with ethyl acetate. The combined extracts were washed with brine and concentrated under reduced pressure. The resulting residue was purified by flash column chromatography eluting with 3:2 ethyl acetate and hexanes to afford 0.370 g (73% yield) of a yellowish solid. ^{1}H NMR (400 MHz, $CDCl_3$): δ 8.81 (s, 1H), 8.51 (d, J = 9.2 Hz, 1H), 8.33 (d, J = 8.4 Hz, 1H), 8.21 (d, J = 9.2 Hz, 1H), 7.48 (d, J = 8.4 Hz, 1H).

(c) 2-({[(1,1-Dimethylethyl)(dimethyl)silyl]oxy}methyl)-6-quinolinamine. To the solution of (6-nitro-2-quinolinyl)methanol (150 mg, 0.74 mmol) and imidazole (101 mg, 1.48 mmol), *tert*-butyldimethylsilyl chloride (143 mg, 0.96 mmol) was added. The resulting mixture was stirred at room temperature for 3 h before water was added to quench the reaction. The reaction mixture was extracted with ether, and the combined extracts were washed with water and brine. After drying with sodium sulfate, the solvent was removed under reduced pressure. The crude product so obtained was then subjected to reduction using Pd/C under 1 atm of hydrogen for 4 h. Filtration over Celite followed by concentration afforded the crude amine, which was directly taken into the next step. ^{1}H NMR (400 MHz, $CDCl_3$): δ 8.63−8.45 (m, 2H), 7.90−7.49 (m, 2H), 7.15−7.25 (m, 1H), 5.38 (s, 1H), 0.90 (s, 9H), 0.08 (s, 6H).

6-(4-Chlorophenyl)-3-[2-(hydroxymethyl)-6-quinolinyl]thieno-[3,2-*d*]pyrimidin-4(3*H*)-one (41). ^{1}H NMR (400 MHz, DMSO-d_6): δ 8.58 (s, 1H), 8.46 (d, J = 8.6 Hz, 1H), 8.20 (s, 1H), 8.09 (d, J = 8.9 Hz, 1H), 8.01 (s, 1H), 7.95−7.88 (m, 4H), 7.77 (d, J = 8.6 Hz, 1H), 7.59 (d, J = 8.5 Hz, 1H), 5.66 (t, J = 6.0 Hz, 1H), 4.77 (d, J = 6.0 Hz, 2H). Elemental analysis was performed for C, H, and N.

6-(4-Chlorophenyl)-3-{2-[(dimethylamino)methyl]-3,4-dihydro-2*H*-1,4-benzoxazin-6-yl}thieno[3,2-*d*]pyrimidin-4 (3*H*)-one (42). ^{1}H NMR (400 MHz, DMSO-d_6): δ 8.35 (s, 1H), 7.96 (s, 1H), 7.93 (d, J = 8.6 Hz, 2H), 7.59 (d, J = 8.6 Hz, 2H), 6.79 (d, J = 8.4 Hz, 1H), 6.68 (d, J = 2.5 Hz, 1H), 6.58 (dd, J = 8.4 and 2.5 Hz, 1H), 6.14 (s, 1H), 4.19 (m, 1H), 3.38 (m, 1H), 3.05 (m, 1H), 2.50 (br s, 2H), 2.25 (s, 6H). Elemental analysis was performed for C, H, and N.

6-(4-Chlorophenyl)-3-[2-[(dimethylamino)methyl]-4-(methylsulfonyl)-3,4-dihydro-2*H*-1,4-benzoxazin-6-yl]thieno[3,2-*d*]pyrimidin-4(3*H*)-one (43). ^{1}H NMR (400 MHz, DMSO-d_6): δ 8.38 (s, 1H), 7.98 (s, 1H), 7.93 (d, J = 8.4 Hz, 2H), 7.76 (s, 1H), 7.58 (d, J = 8.4 Hz, 2H), 7.30 (m, 1H), 7.19 (d, J = 8.8 Hz, 1H), 4.84 (m, 1H), 4.22 (m, 1H), 3.59 (m, 3H), 3.30 (s, 3H), 2.91 (s, 3H), 2.88 (s, 3H). Elemental analysis was performed for C, H, and N.

6-(4-Chlorophenyl)-3-[2-[(dimethylamino)methyl]-4-(phenylsulfonyl)-3,4-dihydro-2*H*-1,4-benzoxazin-6-yl]thieno[3,2-*d*]pyrimidin-4(3*H*)-one (44). (a) [6-Nitro-4-(phenylsulfonyl)-3,4-dihydro-2*H*-1,4-benzoxazin-2-yl]methyl methanesulfonate. To (6-nitro-3,4-dihydro-2*H*-1,4-benzoxazin-2-yl)methyl methanesulfonate (**14**; 1.0 g, 3.47 mmol) in pyridine (5 mL) was added 0.49 mL of benzenesulfonyl chloride (3.81 mmol), and the contents were stirred for 1 h. After addition of water and CH_2Cl_2 to the reaction mixture, the organic layer was separated, dried ($MgSO_4$), and concentrated under vacuum to afford the crude product. Column chromatography with EtOAc/hex (4:1) afforded a red solid 1.42 g (95%). ^{1}H NMR (400 MHz, DMSO-d_6): δ 8.57 (s, 1H), 7.99 (d, J = 9.2 Hz, 1H), 7.78 (m, 3H), 7.62 (m, 2H), 7.16 (d, J = 9.0 Hz, 1H), 4.50 (m, 2H), 4.41 (m, 1H), 3.77 (m, 1H), 3.44 (m, 1H), 3.21 (m, 3H).

(b) *N*,*N*-Dimethyl-1-[6-nitro-4-(phenylsulfonyl)-3,4-dihydro-2*H*-1,4-benzoxazin-2-yl]methanamine. To a solution of [6-nitro-4-(phenylsulfonyl)-3,4-dihydro-2*H*-1,4-benzoxazin-2-yl]methyl methanesulfonate (0.958 g, 2.24 mmol) in THF (10 mL) was added a 2.0 M solution of *N*,*N*-dimethylamine (4.48 mL, 8.96 mmol), and the contents were heated in a sealed tube for 16 h. The reaction was concentrated, followed by addition of EtOAc and satd $NaHCO_3$. Separation of the organic layer and drying ($MgSO_4$), followed by concentration under vacuum, afforded the crude product that was carried on to the next step. ^{1}H NMR (400 MHz, DMSO-d_6): δ 8.58 (s, 1H), 7.99 (d, J = 9.1 Hz, 1H), 7.75 (m, 3H), 7.61 (m, 2H), 7.19 (d, J = 9.1 Hz, 1H), 4.31 (m, 2H), 3.39 (m, 3H), 2.07 (m, 6H).

(c) 2-[(Dimethylamino)methyl]-4-(phenylsulfonyl)-3,4-dihydro-2*H*-1,4-benzoxazin-6-amine. To the crude product obtained in step b above was added 10% Pd/C (0.1 g) and methanol (10 mL), and the contents were kept under hydrogen (40 psi) for 6 h. Filtration through Celite, followed by washing with EtOAc and concentration of the organic layer, gave the amino compound that was carried on to the next step. ^{1}H NMR (400 MHz, DMSO-d_6): δ 7.60 (m, 5H), 6.89 (s,1H), 6.62 (d, J = 8.5 Hz, 1H), 6.24 (d, J = 8.5 Hz, 1H), 4.44 (m, 1H), 4.17 (m, 1H), 3.55 (m, 1H), 2.45 (m, 2H), 2.47 (m, 6H).

6-(4-Chlorophenyl)-3-[2-[(dimethylamino)methyl]-4-(phenylsulfonyl)-3,4-dihydro-2*H*-1,4-benzoxazin-6-yl]thieno[3,2-*d*]pyrimidin-4(3*H*)-one (44). ^{1}H NMR (400 MHz, DMSO-d_6): δ 8.35 (s, 1H), 7.99 (s, 1H), 7.92 (m, 5H), 7.75 (m, 1H), 7.59 (m, 4H), 7.31 (d, J = 8.6 Hz, 1H), 7.31 (d, J = 8.6 Hz, 1H), 7.09 (d, J = 8.8 Hz, 1H), 4.43 (m, 1H), 4.15 (m, 1H), 3.53 (m, 1H), 2.44 (m, 2H), 2.45 (m, 6H). Elemental analysis was performed for C, H, and N.

6-(4-Chlorophenyl)-3-[2-(1-pyrrolidinylmethyl)-3,4-dihydro-2*H*-1,4-benzoxazin-6-yl]thieno[3,2-*d*]pyrimidin-4 (3*H*)-one (45). ^{1}H NMR (400 MHz, DMSO-d_6): δ 8.31 (s, 1H), 7.92 (s, 1H), 7.89 (d, J = 8.6 Hz, 2H), 7.55 (d, J = 8.6 Hz, 2H), 6.76 (d, J = 8.4 Hz, 1H), 6.64 (d, J = 2.5 Hz, 1H), 6.55 (d, J = 8.4 and 2.5 Hz, 1H), 6.09 (s, 1H), 4.15 (m, 1H), 3.36 (m, 1H), 3.04 (m, 1H), 2.46−2.67 (m, 6H), 1.67 (m, 4H). Elemental analysis was performed for C, H, and N.

6-(4-Chlorophenyl)-3-(2-{[(3*R*)-3-hydroxy-1-pyrrolidinyl]-methyl}-3,4-dihydro-2*H*-1,4-benzoxazin-6-yl)thieno[3,2-*d*]pyrimidin-4-(3*H*)-one (46). ^{1}H NMR (400 MHz, DMSO-d_6): δ 8.34 (s, 1H), 7.95 (s, 1H), 7.92 (d, J = 8.6 Hz, 2H), 7.58 (d, J = 8.6 Hz, 2H), 6.79 (d, J = 8.4 Hz, 1H), 6.67 (d, J = 2.5 Hz, 1H), 6.57 (dd, J = 8.4 and 2.5 Hz, 1H), 6.12 (s, 1H), 4.70 (m, 1H), 4.17 (m, 1H), 3.38 (m, 1H), 3.08 (m, 1H), 2.36−2.84 (m, 6H), 1.98 (m, 1H), 1.54 (m, 1H). Elemental analysis was performed for C, H, and N.

6-(4-Chlorophenyl)-3-(2-{[(3*S*)-3-hydroxy-1-pyrrolidinyl]-methyl}-3,4-dihydro-2*H*-1,4-benzoxazin-6-yl)thieno[3,2-*d*]pyrimidin-4-(3*H*)-one (47). ^{1}H NMR (400 MHz, DMSO-d_6): δ 8.34 (s, 1H), 7.96 (s, 1H), 7.93 (d, J = 8.6 Hz, 2H), 7.58 (d, J = 8.6 Hz, 2H), 6.79 (d, J = 8.4 Hz, 1H), 6.67 (d, J = 2.5 Hz, 1H), 6.57 (dd, J = 8.4 and 2.5 Hz, 1H), 6.12 (s, 1H), 4.70 (m, 1H), 4.17 (m, 1H), 3.38 (m, 1H), 3.08 (m, 1H), 2.36−2.84 (m, 6H), 1.98 (m, 1H), 1.54 (m, 1H). Elemental analysis was performed for C, H, and N.

6-(4-Chlorophenyl)-3-[2-(4-morpholinylmethyl)-3,4-dihydro-2*H*-1,4-benzoxazin-6-yl]thieno[3,2-*d*]pyrimidin-4-(3*H*)-one (48). ^{1}H NMR (400 MHz, DMSO-d_6): δ 8.31 (s, 1H), 7.92 (s, 1H), 7.89 (d, J = 8.6 Hz, 2H), 7.55 (d, J = 8.6 Hz, 2H), 6.76 (d, J = 8.4 Hz, 1H), 6.64 (d, J = 2.5 Hz, 1H), 6.54 (dd, J = 8.4 and 2.5 Hz, 1H), 6.10 (s, 1H), 4.21 (m, 1H), 3.56 (t, J = 4.6 Hz, 4H), 3.38 (m, 1H), 3.05 (m, 1H), 2.39−2.53 (m, 6H). Elemental analysis was performed for C, H, and N.

6-(4-Chlorophenyl)-3-{2-[(4-methyl-1-piperazinyl)methyl]-3,4-dihydro-2*H*-1,4-benzoxazin-6-yl}thieno[3,2-*d*]pyrimidin-4-(3*H*)-one (49). ^{1}H NMR (400 MHz, DMSO-d_6): δ 8.34 (s, 1H), 7.95 (s, 1H), 7.92 (d, J = 8.6 Hz, 2H), 7.58 (d, J = 8.6 Hz, 2H), 6.78 (d, J = 8.4 Hz, 1H), 6.67 (d, J = 2.4 Hz, 1H), 6.57 (dd, J = 8.4 and 2.4 Hz, 1H), 6.12 (s, 1H), 4.21 (m, 1H), 3.39 (m, 1H), 3.06 (m, 1H), 2.20−2.58 (m, 10H), 2.16 (s, 3H). Elemental analysis was performed for C, H, and N.

6-(4-chlorophenyl)-3-{2-[(dimethylamino)methyl]-2,3-dihydro-1,4-benzodioxin-6-yl}thieno[3,2-*d*]pyrimidin-4-(3*H*)-one (50). ^{1}H NMR (400 MHz, DMSO-d_6): δ 8.37 (s, 1H), 7.98 (s, 1H), 7.93 (d, J = 8.6 Hz, 2H), 7.59 (d, J = 8.6 Hz, 2H), 7.15 (d, J = 1.8 Hz, 1H), 7.03 (m, 2H), 4.40 (m, 2H), 4.04 (dd, J = 11.5 and 7.0 Hz, 1H), 2.56 (br s, 2H), 2.27 (s, 6H). Elemental analysis was performed for C, H, and N.

6-(4-Chlorophenyl)-3-{(2*S*)-2-[(dimethylamino)methyl]-2,3-dihydro-1,4-benzodioxin-6-yl}thieno[3,2-*d*]pyrimidin-4-(3*H*)-one (51). (a) 2-{[(Methyloxy)methyl]oxy}-5-nitrophenol. To a solution of 4-nitrocatechol **10** (12.7 g, 81.9 mmol) in 100 mL of dry DMF were added potassium carbonate (13.5 g, 97.8 mmol) and chloromethyl methyl ether (6.2 mL, 97.8 mmol) at 40 °C. The

mixture was stirred at that temperature for an hour, and then solvent was removed. Water was added, and the aqueous layer was extracted with ethyl acetate three times. The combined organic layers were washed with brine and dried over magnesium sulfate. Concentration followed by column chromatography on silica gel using a 4:1 mixture of hexane/ethyl acetate afforded 2-{[(methyloxy)methyl]oxy}-5-nitrophenol as a solid (9.4 g, 58%). ^{1}H NMR (400 MHz, $CDCl_3$): δ 7.80 (m, 2H), 7.18 (d, J = 8.8 Hz, 1H), 5.98 (s, 1H), 5.32 (s, 2H), 3.53 (s, 3H).

(b) (2*R*)-2-{[(2-{[(methyloxy)methyl]oxy}-5-nitrophenyl)oxy]methyl}oxirane (11). To a solution of 2-{[(methyloxy)methyl]oxy}-5-nitrophenol (1 g, 5 mmol), triphenylphosphine (3.95 g, 15 mmol), and (*R*)-glycidol (558 mg, 7.5 mmol) in 50 mL of dry DCM was added di-*tert*-butyl azodicarboxylate (3.47 g, 15 mmol) at room temperature. The reaction was stirred at room temperature overnight. Concentration followed by column chromatography on silica gel using hexane/ethyl acetate 4:1 afforded (2*R*)-2-{[(2-{[(methyloxy)methyl]oxy}-5-nitrophenyl)oxy]methyl}oxirane as a solid (0.75 g, 59%). ^{1}H NMR (400 MHz, $CDCl_3$): δ 7.88 (dd, J = 9.0 and 2.5 Hz, 1H), 7.82 (d, J = 2.5 Hz, 1H), 7.22 (d, J = 9.0, 1H), 5.31 (s, 2H), 4.42 (dd, J = 11.3 and 2.6 Hz, 1H), 4.02 (dd, J = 11.3 and 6.0 Hz, 1H), 3.52 (s, 3H), 3.42 (m, 1H), 2.94 (m, 1H), 2.79 (m, 1H).

6-(4-Chlorophenyl)-3-{(2*S*)-2-[(dimethylamino)methyl]-2,3-dihydro-1,4-benzodioxin-6-yl}thieno[3,2-*d*]pyrimidin-4-(3*H*)-one (51). ^{1}H NMR (400 MHz, DMSO-d_6): δ 8.37 (s, 1H), 7.97 (s, 1H), 7.93 (d, J = 8.5 Hz, 2H), 7.59 (d, J = 8.5 Hz, 2H), 7.14 (d, J = 2.0 Hz, 1H), 7.02 (m, 2H), 4.38 (m, 2H), 4.03 (dd, J = 11.4 and 7.0 Hz, 1H), 2.54 (d, J = 6.0 Hz, 2H), 2.25 (s, 6H). Elemental analysis was performed for C, H, and N.

6-(4-Chlorophenyl)-3-{(2*R*)-2-[(dimethylamino)methyl]-2,3-dihydro-1,4-benzodioxin-6-yl}thieno[3,2-*d*]pyrimidin-4-(3*H*)-one (52).

(2*S*)-2-{[(2-{[(methyloxy)methyl]oxy}-5-nitrophenyl)oxy]methyl}oxirane. This intermediate was synthesized by substituting (*S*)-glycidol for (*R*)-glycidol and employing the techniques found for compound **51**. ^{1}H NMR (400 MHz, $CDCl_3$): δ 7.88 (dd, J = 9.0 and 2.6 Hz, 1H), 7.82 (d, J = 2.6 Hz, 1H), 7.22 (d, J = 9.0 Hz, 1H), 5.31 (s, 2H), 4.42 (dd, J = 11.4 and 2.7 Hz, 1H), 4.03 (dd, J = 11.4 and 6.0 Hz, 1H), 3.52 (s, 3H), 3.41 (m, 1H), 2.93 (m, 1H), 2.79 (m, 1H).

6-(4-Chlorophenyl)-3-{(2*R*)-2-[(dimethylamino)methyl]-2,3-dihydro-1,4-benzodioxin-6-yl}thieno[3,2-*d*]pyrimidin-4-(3*H*)-one (52). The title compound was synthesized by substituting (2*R*)-2-[(dimethylamino) methyl]-2,3-dihydro-1,4-benzodioxin-6-amine (the intermediate produced from (2*S*)-2-{[(2-{[(methyloxy)methyl]-oxy}-5-nitrophenyl)oxy]methyl}oxirane (compound **51**, step a, according to patent application WO0121577) for 2-[(dimethylamino)methyl]-2,3-dihydro-1,4-benzodioxin-6-amine and employing the techniques found for compound **16**. ^{1}H NMR (400 MHz, DMSO-d_6): δ 8.37 (s, 1H), 7.97 (s, 1H), 7.93 (d, J = 8.4 Hz, 2H), 7.59 (d, J = 8.4 Hz, 2H), 7.14 (d, J = 2.0 Hz, 1H), 7.02 (m, 2H), 4.38 (m, 2H), 4.03 (dd, J = 11.4 and 7.0 Hz, 1H), 2.54 (d, J = 6.2 Hz, 2H), 2.25 (s, 6H). Elemental analysis was performed for C, H, and N.

6-(4-Chlorophenyl)-3-(2-{[(2*S*)-2-(methoxymethyl)pyrrolidin-1-yl]methyl}-1-methyl-1*H*-indol-5-yl)thieno[3,2-*d*]pyrimidin-4(3*H*)-one hydrochloride (53). (a) 1-{[(2*S*)-6-nitro-2,3-dihydro-1,4-benzodioxin-2-yl]methyl}pyrrolidine. ^{1}H NMR (400 MHz, DMSO-d_6): δ 7.78 (dd, J = 8.9 and 2.8 Hz, 1H), 7.74 (d, J = 2.8 Hz, 1H), 7.10 (d, J = 8.9 Hz, 2H), 4.49 (m, 1H), 4.40 (dd, J = 8.4 Hz and J = 2.4 Hz, 1H), 4.07 (dd, J = 11.7 and 7.0 Hz, 1H), 2.43 (d, J = 6.0 Hz, 2H), 2.22 (s, 5H).

(b) [(2*S*)-2-(1-Pyrrolidinylmethyl)-2,3-dihydro-1,4-benzodioxin-6-yl]amine. (2*S*)-2-(1-pyrrolidinylmethyl)-2,3-dihydro-1,4-benzodioxin-6-amine. ^{1}H NMR (400 MHz, DMSO-d_6): δ 6.52 (d, J = 8.3 Hz, 1H), 6.09 (d, J = 2.6 Hz, 1H), 6.05 (dd, J = 8.3 and 2.6 Hz, 1H), 4.6 (s, 2H), 4.19 (dd, J = 11.3 Hz and J = 2.2 Hz, 1H), 4.11 (m, 1H), 3.83 (dd, J = 11.3 and 7.4 Hz, 1H), 2.41 (d, J = 5.0 Hz, 2H), 2.20 (s, 5H).

6-(4-Chlorophenyl)-3-(2-{[(2*S*)-2-(methoxymethyl)pyrrolidin-1-yl]methyl}-1-methyl-1*H*-indol-5-yl)thieno[3,2-*d*]pyrimidin-4(3*H*)-one hydrochloride (53). The title compound was synthesized using the same procedures as that for 6-(4-chlorophenyl)-3-[1-methyl-2-(pyrrolidin-1-ylmethyl)-1*H*-indol-5-yl]thieno[3,2-*d*]pyrimidin-4(3*H*)-one hydrochloride, using (2*R*)-2-(methoxymethyl)pyrrolidine, instead of pyrrolidine. ^{1}H NMR (400 MHz, $CDCl_3$): δ 12.9 (br s, 1H), 8.6 (s, 1H), 7.80 (s, 1H), 7.68 (d, J = 8.5 Hz, 2H), 7.65 (s, 1H), 7.55 (d, J = 8.8 Hz, 1H), 7.48 (d, J = 8.5 Hz, 2H), 7.30 (d, J = 8.9 Hz, 1H), 6.80 (s, 1H), 4.94 (d, J = 14.3 Hz, 1H), 4.46 (m, 2H), 4.03 (s, 3H), 3.74−3.60 (m, 2H), 3.55 (s, 3H), 3.00 (br s, 2H), 2.28 (br s, 1H), 2.17 (br s, 1H), 1.96 (br s, 2H). Elemental analysis was performed for C, H, and N.

Biological Assays. Reporter Gene Assay. A stable cell line that coexpresses the cloned human MCH R1 and the inducible reporter element Gal4/Elk1-Luc$^+$ was developed by transfecting the CHO Gal4/Elk1-Luc$^+$ host stable cell line with cloned human MCH R1. Clones were selected based on fold response to MCH peptide over basal control. Stock flasks for the CHO Gal4/Elk-1 MCH R1 cell line and host are maintained in T-225 cell culture flasks at 37 °C and 5% CO_2. The stock flasks are split two times per week at a 1:40 split ratio. Cells to be used for the assay are split from the stock flasks. Cells are removed from the flasks with 0.05% trypsin + 0.53 mM EDTA. Two separate cell stocks are maintained weekly. The assay consists of cells plated at 10 000 cells/well in DMEM/F12, 5% FBS, 2 mM L-glutamine in black 96-well assay plates. The day after plating, the media is removed by aspiration 16 h prior to assay, followed by the addition of 90 μL of media without serum to reduce background signal noise. Compounds are prepared by making a stock solution from solid at 3 × 10 to 3 M. The stock solutions are serially diluted 1:3 in 100% DMSO using a Beckman Biomek 2000 as 10 point curves in duplicate. On the day of the assay, the compounds (1 μL) were pipetted into the assay plate using a Beckman Multimek. Following incubation for 45 min at 37 °C, an EC_{80} concentration of MCH (MCH R1) or thrombin (host) is added to the plate, allowing for appropriate controls. The plates are then incubated under the same conditions for 5 h. Under subdued light conditions, the compound/assay solution is removed by aspiration from the plates, followed by the addition of 50 μL of a 1:1 solution containing SteadyGlo and Dulbecco's phosphate buffered saline with 1 mM $CaCl_2$ and 1 mM $MgCl_2$. Plates are sealed with self-adhesive clear plate seals and wiped with a static free dryer sheet to reduce false counts due to static charge. The amount of luciferase generated is quantified in a Packard TopCount with a 2 s per well count time.

hERG Assay. The hERG potassium channels were stably expressed in CHO-K1 cells. The CHO-K1 cells were maintained in cell media that contained 90% Iscove's modified Dulbecco's medium, 10% fetal bovine serum, 1% HT supplement, 1% NEAA, penicillin G sodium 100 units/mL, and streptomycin sulfate 100 μg/mL, and Geneticin 500 μg/mL. Confluent cells in flasks were rinsed once with PBS prior to passage. The flasks were incubated with Versene (EDTA) 1:5000 for 5 min at 37 °C to detach the cells from the flasks. Cells used in electrophysiology experiments were plated on glass coverslips 24 to 48 h prior to use. hERG channels were studied using the whole cell mode of the patch clamp technique.[9] To measure drug effects, the cells were held at −80 mV, then stepped to +20 mV for 400 ms, followed by a second pulse to −40 mV, so that the outward tail current characteristic of hERG could be measured. This pulse protocol was repeated at 10 s intervals as compounds were perfused. The currents were stable for up to 45 min. We measured the hERG tail currents at −40 mV, because no other tail currents were present at this potential in nontransfected cells. The temperature was controlled at 25 ± 0.5 °C for all experiments using a temperature controller from Warner Instruments (SHM-6 multi-line solution heater). The pipet solution contained 145 mM K$^+$aspartate, 11 mM EGTA, 5 mM MgATP, 5 mM NaCl, and 5 mM HEPES, pH 7.3, and the bath solution contained 140 mM NaCl, 4 mM KCl, 2.0 mM $CaCl_2$, 1 mM $MgCl_2$, 10 mM HEPES, and 10 mM D-glucose, pH 7.4.

The stock solutions of 10 mM were prepared in DMSO, and final dilutions were made in the bath solution. The highest DMSO concentration in these experiments was 0.3%. In preliminary

experiments, DMSO concentration of 0.3% had no effect on the hERG potassium currents.

Voltage clamp protocols were generated and analyzed using pClamp9 from Axon Instruments. Results are presented as the mean and standard deviation of the mean.

Supporting Information Available: Description of the synthesis and experimental data for the preparation of compounds **3b**−**3k**, **26a**−**40a**, **45a**−**49a**, **27b**−**40b**, and **45b**−**49b** and elemental analysis/HPLC traces for all compounds. This material is available free of charge via the Internet at http://pubs.acs.org.

References

(1) (a) Kawauchi, H.; Kawazoe, I.; Tsubokawa, M.; Kishida, M.; Baker, B. I. Characterization of melanin-concentrating hormone in chum salmon pituitaries. *Nature* **1983**, *305*, 321−323. (b) Vaughan, J. M.; Fischer, W. H.; Hoeger, C.; River, J.; Vale, W. Characterization of melanin-concentrating hormone from rat hypothalamus. *Endocrinology* **1989**, *125*, 1660−1665. (c) Bittencourt, J. C.; Presse, F.; Arias, C.; Peto, C.; Vaughan, J.; Nahon, J. L.; Vale, W.; Sawchenko, P. E. The melanin-concentrating hormone system of the rat brain: an immuno- and hybridization histochemical characterization. *J. Comput. Neurol.* **1992**, *319*, 218−245. (d) Chambers, J.; Ames, R. S.; Bergsma, D.; Muir, A.; Fitzgerald, L. R.; Hervieu, G.; Dytko, G. M.; Foley, J. J.; Martin, J.; Liu, W. S.; Park, J.; Ellis, C.; Gangulay, S.; Konchar, S.; Cluderray, J.; Leslie, R.; Wilson, S.; Sarau, H. M. Melanin-concentrating hormone is the cognate ligand for the orphan G-protein-coupled receptor SLC-1. *Nature* **1999**, *400*, 261−265. (e) Tan, C. P.; Sano, H.; Iwaasa, H.; Pan, J.; Sailer, A. W.; Hreniuk, D. L.; Feighner, S. D.; Palyha, O. C.; Pong, S. S.; Figueroa, D. J.; Austin, C. P.; Jiang, M. M.; Yu, H.; Ito, H.; Ito, J.; Ito, M.; Guan, X. M.; MacNeil, D. J.; Kanatani, A.; Van der Ploeg, L. H.; Howard, A. D. Melanin-concentrating hormone receptor subtypes 1 and 2: Species-specific gene expression. *Genomics* **2002**, *79* (6), 785−92. (f) Hawes, B. E.; Kil, E.; Green, B.; O'Neil, K.; Fried, S.; Graziano, M. P. The melanin-concentrating hormone receptor couples to muntiple G proteins to activate diverse intracellular signaling pathways. *Endocrinology* **2000**, *141*, 4524−32. (g) An, S.; Cutler, G.; Zhao, J. J.; Huang, S. G.; Tian, H.; Li, W.; Liang, L.; Rich, M.; Bakleh, A.; Du, J.; Chen, J. L.; Dai, K. Identification and characterization of a melanin-concentrating hormone receptor. *Proc. Natl. Acad. Sci. U.S.A.* **2001**, *98*, 7576−81. (h) Hill, J.; Duckworth, M.; Murdock, P.; Rennie, G.; Sabido-David, C.; Ames, R. S.; Saito, Y.; Nothacker, H. P.; Wang, Z.; Lin, S. H.; Leslie, F.; Civelli, O. Molecular characterization of the melanin-concentrating hormone receptor. *Nature* **1999**, *400* (6741), 265−9. (i) Sailer, A. W.; Sano, H.; Zeng, Z.; McDonald, T. P.; Pan, J.; Pong, S. S.; Feighner, S. D.; Tan, C. P.; Fukami, T.; Iwaasa, H.; Hreniuk, D. L.; Morin, N. R.; Sadowski, S. J.; Ito, M.; Bansal, A.; Ky, B.; Figueroa, D. L.; Jiang, Q.; Austin, C. P.; MacNeil, D. J.; Ishihara, A.; Ihara, M.; Kanatani, A.; Van der Ploeg, L. H.; Howard, A. D.; Liu, Q. Identification and characterization of a second melanin-concentrating hormone receptor, MCH-2R. *Proc. Natl. Acad. Sci. U.S.A.* **2001**, *98*, 7564−7569.

(2) (a) Shimada, M.; Tritos, D.; Aitken, A.; Donella-Deana, A.; Hemmings, B. A.; Parker, P. J. Mice lacking melanin-concentrating hormone are hypophagic and lean. *Nature* **1998**, *396*, 670−674. *Eur. J. Biochem.* **1982**, *124*, 21. (b) Chen, Y.; Hu, C.; Hsu, C. K.; Zhang, Q.; Bi, C.; Asnicar, M.; Hsiung, H. M.; Fox, N.; Slieker, L. J.; Yang, D. D.; Heiman, M. L.; Shi, Y, Targeted disruption of the melanin-concentrating hormone receptor-1 results in hyperphagia and resistance to diet-induced obesity. *Endocrinology* **2002**, *143*, 2469−2477. (c) Marsh, D. J.; Weingarth, D. T.; Novi, D. E.; Chen, H. Y.; Trumbauer, M. E.; Chen, A. S.; Guan, X. M.; Jiang, M. M.; Feng, Y.; Camacho, R. E.; Shen, Z.; Frazier, E. G.; Yu, H.; Metzger, J. M.; Kuca, S. J.; Shearman, L. P.; Gopal-Truter, S.; Macneil, D. J.; Strack, A. M.; MacIntyre, D. E.; Van der Ploeg, L. H.; Qian, S. Melanin-concentrating hormone 1 receptor-deficient mice are lean, hyperactive, and hyperphagic and have altered metabolism. *Proc. Natl. Acad. Sci. U.S.A.* **2002**, *99*, 3240−3245. (d) Viale, A.; Ortola, C.; Hervieu, G.; Furuta, M.; Barbero, P.; Steiner, D. F.; Seidah, N. G.; Nahon, J. L. Cellular localization and role of prohormone convertases in the processing of pro-melanin-concentrating hormone in mammals. *J. Biol. Chem.* **1999**, *274*, 6536−6545. (e) Gonzolez, M. I.; Vaziri, S.; Wilson, C. A. Behavioral effects of α-MSH and MCH after central administration in the female rat. *Peptides* **1996**, *17*, 171−177. (f) Ludwig, D. S.; Tritos, N. A.; Mastaitis, J. W.; Kulkarni, R.; Kokkotou, E.; Elmquis, J.; Lowell, B.; Flier, J. S.; Maratos-Flier, E. Melanin-concentrating hormone overexpression in transgenic mice leads to obesity and insulin resistance. *J. Clin. Invest.* **2001**, *107*, 379−386. (g) Segal-Lieberman, G.; Bradley, R. L.; Kokkotou, E.; Carlson, M.; Trombly, D. J.; Wang, X.; Bates, S.; Myers, M. G., Jr.; Flier, J. S.; Maratos-Flier, E. Melanin-concentrating hormone is a critical mediator of the leptin-deficient phenotype. *Proc. Natl. Acad. Sci. U.S.A.* **2003**, *100* (17), 10085−10090.

(3) (a) Stricker-Krongrad, A.; Dimitrov, T.; Beck, B. Central and pheripheral dysregulation of melanin-concentrating hormone in obese zucker rats. *Brain Res. Mol. Brain Res.* **2001**, *92* (1−2), 43−48. (b) Qu, D.; Ludwig, D. S.; Gammeltoft, S.; Piper, M.; Pelleymounter, M. A.; Cullen, M. J. A role for melanin-concentrating hormone in the central regulation of feeding behaviour. *Nature* **1996**, *380*, 243−247. (c) Sahu, A. Leptin decreases food intake induced by melanin-concentrating hormone (MCH), galanin (GAL), and neuropeptide Y (NPY) in the rat. *Endocrinology* **1998**, *139*, 4739−4742. (d) Gomori, A.; Ishihara, A.; Ito, M.; Mashiko, S.; Matsushita, H.; Yumoto, M.; Tanaka, T.; Tokita, S.; Moriya, M.; Iwaasa, H.; Kanatani, A. Chronic intracerebroventricular infusion of MCH causes obesity in mice. *Am. J. Physiol. Endocrinol. Metab.* **2003**, *284* (3), E583−588. (e) Ito, M.; Gomori, A.; Ishihara, A.; Oda, Z.; Mashiko, S.; Matsushita, H.; Yumoto, M.; Sano, H.; Moriya, M.; Kanatani, A. Characterization of MCH-mediated obesity in mice. *Am. J. Physiol. Endocrinol. Metab.* **2003**, *284* (5), E940−945. (f) Kennedy, A. R.; Todd, J. F.; Stanley, S. A.; Abbott, C. R.; Small, C. J.; Ghatei, M. A.; Bloom, S. R. Melanin-concentrating hormone (MCH) suppresses thyroid stimulating hormone (TSH) release, in vivo and in vitro, via the hypothalamus and the pituitary. *Endocrinology* **2001**, *142* (7), 3265−3268. (g) Shearman, L. P.; Camacho, R. E.; Sloan, S. D.; Zhou, D.; Bednarek, M. A.; Hreniuk, D. L.; Feighner, S. D.; Tan, C. P.; Howard, A. D.; Van der Ploeg, L. H.; MacIntyre, D. E.; Hickey, G. J.; Strack, A. M. Chronic MCH-1 receptor modulation alters appetite, body weight, and adiposity in rats. *Eur. J. Pharmacol.* **2003**, *15*, *475* (1−3), 37−47. (h) Abbott, C. R.; Kennedy, A. R.; Wren, A. M.; Rossi, M.; Murphy, K. G.; Seal, L. J.; To, J. F.; Ghatei, M. A.; Small, C. J.; Bloom, S. R. Identification of hypothalamic nuclei involved in the orexigenic effect of melanin-concentrating hormone. *Endocrinology* **2003**, *144* (9), 3943−3949. (i) Chaffer, C. L.; Morris, M. J. The feeding response to melanin-concentrating hormone is attenuated by antagonism of NPY Y(1)-receptor in the rat. *Endocrinology* **2002**, *143* (1), 191−197. (j) Rossi, M.; Beak, S. A.; Choi, S. J.; Morgan, D. G.; Ghatei, M. A.; Smith, D. M.; Bloom, S. R. Investigation of the feeding effects of melanin-concentrating hormone on food intake-action independent of galanin and the melanocortin receptors. *Brain Res.* **1999**, *846* (2), 164−170. (k) Guan, J. L.; Uehara, K.; Lu, S.; Wang, Q. P.; Funahashi, H.; Sakurai, T.; Yanagizawa, M.; Shioda, S. Reciprocal synaptic relationships between orexin- and melanin-concentrating hormone-containing neurons in the rat lateral hypothalamus: a novel circuit implicated in feeding regulation. *Int. J. Obes. Relat. Metab. Disord.* **2002**, *26* (12), 1523−1532. (l) Tadayyon, M.; Welters, H. J.; Haynes, A. C.; Cluderay, J. E.; Hervieu, G. Expression of melanin-concentrating hormone receptors in insulin-producing cells: MCH stimulates insulin release in RINm5F and CRI-GI cell-lines. *Biochem. Biophys. Res. Commun.* **2000**, *275*, 709−712. (m) Bradley, R. L.; Mansfield, J. P.; Maratos-Flier, E.; Cheatham, B. Melanin-concentrating hormone activates signaling pathways in 3T3-L1 adipocytes. *Am. J. Physiol. Endocrinol. Metab.* **2002**, *283* (3), E584−592.

(4) (a) Astrand, A.; Bohlooly, Y. M.; Larsdotter, S.; Mahlapuu, M.; Andersen, H.; Tornell, J.; Ohlsson, C.; Snaith, M.; Morgan, D. G. Mice lacking melanin-concentrating hormone receptor 1 demonstrate increased heart rate associated with altered autonomic activity. *Am. J. Physiol. Regul. Integr. Comput. Physiol.* **2004**, *287* (4), R749−758. (b) Bohlooly, Y. M.; Mahlapuu, M.; Anderson, H.; Astrand, A.; Hjorth, S.; Svensso, L.; Tornell, J.; Snaith, M. R.; Morgan, D. G.; Ohlsson, C. Osteoporosis in MCHR1-deficient mice. *Biochem. Biophys. Res. Commun.* **2004**, *318* (4), 946−949. (c) Gibson, W. T.; Pissios, P.; Trombly, D. J.; Luan, J.; Keogh, J.; Wareham, N. J.; Maratos-Flier, E.; O'Rahilly, S.; Farooqi, I. S. Melanin-concentrating hormone receptor mutations and human obesity: functional analysis. *Obes. Res.* **2004**, *12* (5), 743−749. (d) Hawes, B. E.; Green, B.; O'Neill, K.; Arreaza, M. G.; Qiu, P.; Simon, J. S. Identification and characterization of single-nucleotide polymorphisms in MCH-R1 and MCH-R2. *Obes. Res.* **2004**, *12* (8), 1327−1334.

(5) (a) Ludwig, D. S.; Mountjoy, K. G.; Tatro, J. B.; Gillette, J. A.; Frederich, R. C.; Flier, J. S.; Maratos-Flier, E. Melanin-concentrating hormone: a functional melanocortin antagonist in the hypothalamus. *Am. J. Physiol.* **1998**, E627−633. (b) Audinot, V.; Beauverger, P.; Lahaye, C.; Suply, T.; Rodriguez, M.; Ouvry, C.; Lamamy, V.; Imbert, J.; Rique, H.; Nahon, J.-L.; Galizzi, J. P.; Canet, E.; Levens, N.; Fauchere, J. L.; Boutin, J. A. Structure activity relationship studies of melanin-concentrating hormone (MCH)-related peptide ligands at SLC-1, the human MCH receptor. *J. Biol. Chem.* **2001**, *276*, 13554−13562. (c) Bednarek, M. A.; Hreniuk, D. L.; Tan, C.; Palyha, O. C.; MacNeil, D. J.; Van der Ploeg, L. H. Y.; Howard, A. D.; Feighner, S. D. Synthesis and biological evaluation in vitro of selective, high

affinity peptide antagonists of human melanin-concentrating hormone action at human melanin-concentrating hormone receptor 1. *Biochemistry* **2002**, *41*, 6383−6390. (d) Shearman, L. P.; Camacho, R. E.; Stribling, D. S.; Zhou, D.; Bednarek, M. A.; Hreniuk, D. L.; Feighner, S. D.; Tan, C. P.; Howard, A. D.; Van der Ploeg, L. H. T.; MacIntyre, D. E.; Hickey, G. J.; Strack, A. M. Chronic MCH-1 receptor modulation alters appetite, body weight, and adiposity in rats. *Eur. J. Pharmacol.* **2003**, *475*, 37−47. (e) Takekawa, S.; Asami, A.; Ishihara, Y.; Terauchi, J.; Kato, K.; Shimomura, Y.; Mori, M.; Murakoshi, H.; Kato, K.; Suzuki, N.; Nishimura, O.; Fujino, M. T-226296: a novel, orally active and selective melanin-concentrating hormone receptor antagonist. *Eur. J. Pharmacol.* **2002**, *438* (3), 129−135. (f) Kowalski, T. J.; Farley, C.; Cohen-Williams, M. E.; Varty, G.; Spar, B. D. Melanin-concentrating hormone-1 receptor antagonism decreases feeding by reducing meal size. *Eur. J. Pharmacol.* **2004**, *497*, 41−47. (g) Borowsky, B.; Durkin, M. M.; Ogozalek, K.; Marzabadi, M. R.; DeLeon, J.; Lagu, B.; et al. Antidepressant, anxiolytic, and anorectic effects of a melanin-concentrating hormone-1 receptor antagonist. *Nat. Med.* **2002**, *8*, 825−830. (h) Arienzo, R.; Clark, D. E.; Cramp, S.; Daly, S.; Dyke, H. J.; Lockey, P.; Norman, D.; Roach, A. G.; Stuttle, K.; Tomlinson, M.; Wong, M.; Wren, S. P. Structure−activity relationships of a novel series of melanin-concentrating hormone (MCH) receptor antagonists. *Bioorg. Med. Chem. Lett.* **2004**, *14*, 4099−4102. (i) Clark, D. E.; Higgs, C.; Wren, S. P.; Dyke, H. J.; Wong, M.; Norman, D.; Lockey, P.; Roach, A. G. A virtual screening approach to finding novel and potent antagonist at the melanin-concentrating hormone 1 receptor. *J. Med. Chem.* **2004**, *47*, 3962−3971. (j) Souers, A. J.; Wodka, D.; Gao, J.; Lewis, J. C.; Vasudevan, A.; Gentles, R.; Brodjian, S.; Dayton, B.; Ogiela, C. A.; Fry, D.; Hernandez, L. E.; Marsh, K. C.; Collins, C. A.; Kym, P. R. Synthesis and evaluation of 2-amino-8-alkoxy quinolines as MCHr1 antagonists. Part 1. *Bioorg. Med. Chem. Lett.* **2004**, *14*, 4873−4877. (k) Vasudevan, A.; Wodka, D.; Verzal, M. K.; Souers, A. J.; Gao, J.; Brodjian, S.; Fry, D.; Dayton, B.; Marsh, K. C.; Hernandez, L. E.; Ogiela, C. A.; Collins, C. A.; Kym, P. R. Synthesis and evaluation of 2-amino-8-alkoxy quinolines as MCHr1 antagonists. Part 2. *Bioorg. Med. Chem. Lett.* **2004**, *14*, 4879−4882. (l) Souers, A. J.; Wodka, D.; Gao, J.; Lewis, J. C.; Vasudevan, A.; Brodjian, S.; Dayton, B.; Ogiela, C. A.; Fry, D.; Hernandez, L. E.; Marsh, K. C.; Collins, C. A.; Kym, P. R. Synthesis and evaluation of 2-amino-8-alkoxy quinolines as MCHr1 antagonists. Part 3. *Bioorg. Med. Chem. Lett.* **2004**, *14*, 4883−4886. (m) Ulven, T.; Frimurer, T. M.; Receveur, J.-M.; Little, P. B.; Rist, O.; Norregaard, P. K.; Hogberg, T. 6-Acylamino-2-aminoquinolines as potent melanin-concentrating hormone 1 receptor antagonist. Identification, structure−activity relationship, and investigation of binding mode. *J. Med. Chem.* **2005**, *48*, 5684−5697.

(6) (a) Vasudevan, A.; Verzal, M. K.; Wodka, D.; Souers, A. J.; Blackburn, C.; Che, J. L.; Lai, S.; Brodjian, S.; Falls, D. H.; Dayton, B. D.; Govek, E.; Daniels, T.; Geddes, B.; Marsh, K. C.; Hernandez, L. E.; Collins, C. A.; Kym, P. R. Identification of aminopiperidine benzamides as MCHr1 antagonists. *Bioorg. Med. Chem. Lett.* **2005**, *15*, 3412−3416. (b) Palani, A.; Shapiro, S.; McBriar, M. D.; Clader, J. W.; Greenlee, W. J.; Spar, B.; Kowalski, T. J.; Farley, C.; Cook, J.; van Heek, M.; Weig, B.; O'Neill, K.; Graziano, M.; Hawes, B. Biaryl ureas as potent and orally efficacious melanin-concentrating hormone receptor 1 antagonists for the treatment of obesity. *J. Med. Chem.* **2005**, *48*, 4746−4749. (c) Souers, A. J.; Gao, J.; Wodka, D.; Judd, A. S.; Mulhern, M. M.; Napier, J. J.; Brune, M. E.; Bush, E. N.; Brodjian, S. J.; Dayton, B. D.; Shapiro, R.; Hernandez, L. E.; Marsh, K. C.; Sham, H. L.; Collins, C. A.; Kym, P. R. Synthesis and evaluation of urea-based indazoles as melanin-concentrating hormone receptor 1 antagonists for the treatment of obesity. *Bioorg. Med. Chem. Lett.* **2005**, *15*, 2752−2757. (d) Chaki, S.; Funakoshi, T.; Hirota-Okuno, S.; Nishiguchi, M.; Shimazaki, T.; Iijima, M.; Grottick, A. J.; Kanuma, K.; Omodera, K.; Sekiguchi, Y.; Okuyama, S.; Tran, T.; Semple, G.; Thomsen, W. Anxiolytic- and antidepressant-like profile of ATC0065 and ATC0175: Nonpeptidic and orally active melanin-concentrating hormone receptor 1 antagonists. *J. Pharm. Exp. Ther.* **2005**, *313*, 831−839. (e) Souers, A. J.; Gao, J.; Brune, M.; Bush, E.; Wodka, D.; Vasudevan, A.; Judd, A. S.; Mulhern, M.; Brodjian, S.; Dayton, B.; Shapiro, R.; Hernandez, L. E.; Marsh, K. C.; Sham, H. L.; Collins, C. A.; Kym, P. R. Identification of 2-(4-benzyloxyphenyl)-*N*-[1-(2-pyrrolidin-1-yl-ethyl)-1*H*-indazol-6-yl]acetamide, an orally efficacious melanin-concentrating hormone receptor antagonist for the treatment of obesity. *J. Med. Chem.* **2005**, *48*, 1318−1321. (f) Kym, P. R.; Iyengar, R.; Souers, A. J.; Lynch, J. K.; Judd, A. S.; Gao, J.; Freeman, J.; Mulhern, M.; Zhao, G.; Vasudevan, A.; Wodka, D.; Blackburn, C.; Brown, J.; Che, J. L.; Cullis, C.; Lai, S. J.; LaMarche, M. J.; Marsilje, T.; Roses, J.; Sells, T.; Geddes, B.; Govek, E.; Patane, M.; Fry, D.; Dayton, B. D.; Brodjian, S.; Falls, D.; Brune, M.; Bush, E.; Shapiro, R.; Knourek-Segel, V.; Fey, T.; McDowell, C.; Reinhart, G. A.; Preusser, L. C.; Marsh, K.; Hernandez, L.; Sham, H. L.; Collins, C. A. Discovery and characterization of aminopiperidinecoumarin melanin-concentrating hormone receptor 1 antagonists. *J. Med. Chem.* **2005**, *48*, 5888−5891. (g) McBriar, M. D.; Guzik, H.; Xu, R.; Paruchova, J.; Li, S.; Palani, A.; Clader, J. W.; Greenlee, W. J.; Hawes, B. E.; Kowalski, T. J.; O'Neill, K.; Spar, B.; Weig, B. Discovery of bicycloalkyl urea melanin-concentrating hormone receptor antagonist: orally efficacious antiobesity therapeutics. *J. Med. Chem.* **2005**, *48*, 2274−2277. (h) Collins, C. A.; Kym, P. R. Prospects for obesity treatment: MCH receptor antagonists. *Curr. Opin. Invest. Drugs* **2003**, *4*, 386-394. (i) Carpenter, A. J.; Hertzog, D. L. Melanin-concentrating hormone receptor antagonists as potential antiobesity agents. *Expert Opin. Ther. Pat.* **2002**, *12*, 1639−1646.

(7) Liu, P.; Chen Y.; Deng J.; Tu, Y. An efficient method for the preparation of benzylic bromides. *Synthesis* **2001**, *14*, 2078−2080.

(8) Thomas, L.; Reichl, R.; Mueller, S. G.; Stenkamp, D.; Schindler, M. A novel MCH-1R antagonist reduces body weight in Rhesus monkeys. NAASO meeting, 2005, P2−224.

(9) Kato, K.; Terauchi, J.; Mori, M.; Suzuki, N.; Shimomura, Y.; Takekawa, S.; Ishihara, Y. Patent WO 01/21577 A2, 2001.

(10) pK_a values were calculated using Advanced Chemistry Development (ACD/Labs) software.

(11) Hammil, O. P.; Marty, A.; Neher, E.; Sakmann, B.; Sigworth, F. Improved patch-clamp techniques for high-resolution recording from cells and cell-free patches. *Pflugers Arch.* **1981**, *391*, 85−100.

JM060572F